

Spatial variation of coke quality in the non-recovery beehive coke ovens

by

Magrieta Segers

Submitted in partial fulfillment of the requirements for the degree

MASTER OF SCIENCE

In the Faculty of Natural & Agricultural Science

University of Pretoria

Pretoria

October 2004

ABSTRACT

More than 50% of hot metal production worldwide takes place in blast furnaces. Coke is the most expensive raw material in the blast furnace. It acts as the burden support as well as heat source and reductant in the blast furnace. As technology advances, supplementary fuels can supply heat and reduce the iron oxides, but coke would always be needed as burden support. Blast furnaces have been using coke for the past century and will continue to use coke for the next few decades. The price of coke is determined by its quality. Strict environmental laws and regulations in the USA pushed coke-making technology since the early 1990s towards the beehive type of oven. Gas collected during the coke cycle is used to supply heat to the process.

The aim of this study is to investigate the spatial variation and coke quality in the non-recovery ovens and provide an explanation for it. The original coal was tested and samples of the coke were obtained from the top, bottom and sides of a coke oven. The samples were prepared and submitted for image analysis to determine the porosity, cell wall thickness and pore diameter. The samples were also submitted for a microscopical point counting to determine the micro textures of the coke. The coke was further submitted for the coke strength after reaction testing (CSR).

The results show clear variation in the coke and a model of the behavior of the gas inside the coke oven during the carbonization process was developed based on the results of the tests. The model shows the flow of gas from the bottom of the oven up along the sidewalls to escape from the coke charge through the top. The flow of gas enriched the coke on the side of the oven by deposition of pyrolytic carbon to create an ultra-high grade of coke that could physically be separated from the rest of the coke and be sold separately at a higher price.

TABLE OF CONTENTS

ABSTRACT.....	ii
LIST OF ILLUSTRATIONS.....	v
LIST OF TABLES.....	vii
1. INTRODUCTION	1
1.1. The importance of the coke industry	2
1.2. Environmental problems related to carbonization and the coke utilization ...	5
2. LITURATURE STUDY	8
2.1. History of beehive coke ovens	8
2.2. Operation of beehive ovens	12
2.3. Plastic zone and gas flow	13
2.4. The future of coke ovens in the USA.....	15
3. PROBLEM STATEMENT	15
Problem statement background	15
4. EXPERIMENTAL METHODS.....	17
4.1. Sampling.....	17
4.2. Sample preparation for petrography.....	21
4.3. Analysis on coal	24
4.3.1. Volatile matter and moisture content.....	24
4.3.2. Ash.....	25
4.3.3. Fixed carbon	26
4.3.4. Sulfur	27
4.3.5. Calorific value.....	27

4.3.6. Alkalis.....	28
4.3.7. Free swelling index.....	28
4.3.8. Gieseler plasticity test.....	28
4.3.9 Hardgrove grindability.....	29
4.3.10 Size analysis.....	30
4.3.11 Ash fusion temperature.....	30
4.3.12 Coal rank.....	31
4.3.13 Maceral analysis	32
4.3.14 Composition balance index.....	32
4.4. Analysis on Coke	33
4.4.1. Coke reactivity index and coke strength after reaction.....	33
4.4.2 Sample preparation for microscopical analysis	35
4.4.3. Structure.....	37
4.4.4. Texture	40
5. RESULTS.....	41
5.1. Analytical test results on coal.....	41
5.2. Results of the structural analysis on coke	44
5.2.1. Coke piece T	44
5.2.2. Coke piece S	50
5.2.3. Coke piece B.....	55
5.3. Results of the texture analysis on coke	60
5.4. Results of the CSR test on coke	61
6. DISCUSSION	61
6.1. Results of the structural analysis.....	61
6.2. Results of the texture analysis.....	67
6.3. CSR results.....	68
6.4. Coke oven model.....	69
7. CONCLUSIONS	71

LIST OF ILLUSTRATIONS

Figure 1: Vansant coke plant in Virginia..... 9

Figure 2: Jewell Thompson heat recovery coke oven 10

Figure 3: Indiana Harbor Coke Plant on the shores of Lake Michigan in Gary..... 11

Figure 4: .The waste heat used for steam production to generate 87 MW of electricity.... 12

Figure 5: Coke guide with massive sample as retracted from the oven..... 18

*Figure 6: The coke taken from the top of the coke bed was marked T, from the side, S and
from the bottom B..... 19*

Figure 7: Appearance of coke piece T from the top of the coke bed..... 19

Figure 8: Close up of coke piece B from the bottom of the coke bed..... 20

Figure 9: Appearance of coke piece S from the side of the coke bed..... 20

Figure 10: (a) Coke piece “ T” from the top of the coke bed; 20” (app. 51cm) long..... 21
(b) Coke piece “ S” from the side of the coke bed; 19.25” (app. 49cm) long..... 21
(c) Coke piece “ B” from the bottom of the coke bed; 12” (app. 31 cm) long... 21

*Figure 11: Schematic plan for cutting up large coke pieces into layers, starting in the
cauliflower en and using the labels with alpha characters, starting at layer A... 22*

*Figure 12: A schematic plan to cut each layer into individual samples. Starting in the
back left corner, the first sample was labeled as 1, the one in front of it is
labeled as 1.2 and the one to the right of it the number 2 23*

*Figure 13: Microscope and computer set up with automatic stage and stepper motors for
scanning the coke..... 37*

Figure 14: Microscope image of coke. Pores dark grey to black and coke cell walls white. 38

*Figure 15: Image on the computer screen while scanning the coke structure. Blue and red
colours represent the pores. The yellow lines represent the measurement of
the cell wall thickness in a vertical and horizontal direction..... 39*

Figure 16: Structural properties of coke piece T..... 47

Figure 17: Descriptive statistics of porosity of coke piece T..... 48

Figure 18: Descriptive statistics of pore diameter of coke piece T..... 48

Figure 19: Descriptive statistics of cell wall thickness of coke piece T 49

Figure 20: Structural properties of coke piece S..... 52

Figure 21: Descriptive Statistics of the Porosity of Coke piece S..... 53

<i>Figure 22: Descriptive statistics of the pore diameter of coke piece S.....</i>	53
<i>Figure 23: Descriptive statistics of the cell wall thickness of coke piece S.....</i>	54
<i>Figure 24: Structural properties of coke piece B.....</i>	58
<i>Figure 25: Descriptive statistics of porosity of coke piece B.....</i>	58
<i>Figure 26: Descriptive statistics of pore diameter of coke piece B.....</i>	59
<i>Figure 27: Descriptive statistics of cell wall thickness of coke piece</i>	59
<i>Figure 28: Mean porosity results for the cauliflower and tar zones in each coke piece.....</i>	62
<i>Figure 29: Box plots of porosity of the 3 coke pieces.....</i>	63
<i>Figure 30: Pore diameter results of the 3 coke pieces.....</i>	64
<i>Figure 31: Box plot of the cell wall thickness of each coke piece investigated.....</i>	65
<i>Figure 32: Cell wall thickness as represented by the mean value of each zone of each coke piece investigated</i>	66
<i>Figure 33: Box plot of the pore diameter of each coke piece investigated.....</i>	67
<i>Figure 34: CSR, Porosity and pyrolytic carbon results.....</i>	68
<i>Figure 35: Suggested coke oven model with the flow of gas. Gas cannot flow through the plastic zone and is forced from the bottom of the oven up on the sides of the oven.....</i>	70

LIST OF TABELS

Table 1: Sample distribution.	24
Table 2: Grinding parameters.	36
Table 3: Polishing parameters	36
Table 4: Results of Jewell Smokeless Coal.	41
Table 5: Structural properties of coke sample from the top of coke bed the oven: Coke piece T (x is the value and s the standard deviation)	44
Table 6: Structural properties of coke sample from the side of the coke bed in the oven: Coke piece S (x is the value and s the standard deviation)	50
Table 7: Structural properties of coke sample from the bottom of the coke bed in the oven: Coke piece B (x is the value and s the standard deviation)	55
Table 8: Summary of structure results	60
Table 9: Texture results of coke pieces T, S and B.....	60
Table 10: CSR results	61

1. INTRODUCTION

Worldwide, more than 50% of all hot metal production takes place in blast furnaces, using coke, and experts predict that it will not change for the next few decades in spite of the availability of any newer and more advanced iron and steel making technology.

Coke is still the best raw material to use in blast furnaces and coke production continues to be of prime importance in iron making. It is irreplaceable as a fuel, reductant and burden support, all in one product. Supplementary fuels can supply heat and reduce the iron oxides but cannot support the burden of iron and limestone in the furnace. Thus, there is a continued need for a minimum quantity of very high quality coke as long as blast furnaces operate.

The continued operation of larger blast furnaces and larger coke ovens in the iron and steel industry throughout the world has created the demand for higher quality coke at optimized cost and minimum pollution.

There are mainly two types of coke ovens: By-product and non-recovery type of ovens. By-product ovens are normally slot ovens and the non-recovery ovens are normally Beehive type designs. The slot ovens are normally tall, narrow silica-brick chambers. Coal is loaded from the top and is heated mainly from the sides by fuel gas in flues built into the walls of the ovens. 10-100 ovens are grouped together in a battery. The ovens are run under high pressure and are associated with air pollution as emissions leak into the atmosphere through the door or loading holes. Gas, oils and tars are collected during the coking process and directed to a by-product plant. The by-product plants are complex and have poor profit margins. The Clean Air Act of 1990 redirected the development of coke making in the USA to the non-recovery coke making technology. They are normally

rectangular beehive shaped. Sometimes gas is recovered during the coking cycle to be burned to supply heat to the process (Walters, 1999).

1.1 The importance of the coke industry

The coke industry is burdened with costly operating and environmental problems resulting in strict environmental regulations from government agencies. In the past 30 years, little new technology or break-through designs have been developed by the coke industry. This makes the steel industry reluctant to invest in new coke making facilities and large amounts of money have been invested to seek alternative processes of making steel without using coke. Processes like the Corex and the Direct Reduction, Pulverized Coal Injection (PCI) and stamp charging of charcoal all have merit, but the steel industries all around the world are still heavily dependent on coke. The bulk of the steel produced is still from blast furnaces (Gray 1997).

During the coking process, the oven is heated from the sides or top and bottom, depending on the process design, and the coal closest to the heating zone of the oven goes through the coal-to-coke phase (plastic zone). The plastic zone then moves inward away from the oven walls until the whole charge has been coked. Since the coke starts forming against the walls, most of the gas emitted from the coal travels through the cracks and openings in the coke closest to the walls of the oven. Some of the tars and oils are deposited in thermally formed cracks (fissures) and due to thermal cracking contribute to the deposition of pyrolytic carbon in these openings. Increased pyrolytic carbon deposition tends to decrease the coke reactivity index (CRI) and consequently increase the coke strength after reaction (CSR). Therefore, coke of the highest quality is formed against the side wall (heating zones) in the conventional coke oven (Arendt et al. 1999).

Coke is the most expensive raw material in the steel making process. The better the quality of the coke, the more expensive it becomes. However, the better the coke quality, the

smaller the quantity of coke needed to produce a constant unit of steel, especially since it can be supplemented with pulverized coal injection (PCI) into the blast furnace. Although the PCI process supplements the use of coke, it cannot supplant it. In theory up to 40% of the coke charge can be replaced by coal injection. The success of the higher level of coal injection depends on the use of better quality coke. Thus, even with PCI, blast furnaces will always require at least a minimum amount of very high quality coke (Price et al. 1997).

The properties that qualify a coke as acceptable for utilization in the blast furnace depend on the type and size of the furnace. The control limits are constantly getting tighter as the quality of the coke has improved in recent years.

The quality of the coke is a function of both the physical and chemical properties. According to Poveromo (1997), the physical requirements are:

- a. Burden support: One of the most important parameters of the coke in the blast furnace is to support its own weight plus the weight of the iron ore and limestone on top of it. That means that the coke must be physically strong. In terms of coke petrography, this implies small pores and thick cell walls. The CSR value is also an indication of the physical strength of the coke.
- b. Permeability: The open spaces between coke pieces must be large enough to allow the gas to travel readily through the coke bed. The permeability of the coke burden must be at least seven times higher than that of the burden of the iron ore. Traditionally, blast furnace operators prefer a uniform coke size in order to control the gas flow in the furnace as the size distribution of the coke also plays a role in the permeability. A narrow size distribution prevents size segregation, and finer coke decreases permeability.

- c. Grindability: The coke must have a high resistance to abrasion (a low grindability) to be able to withstand handling and transportation between the coke ovens and the blast furnace, and abrasion within the blast furnace itself.

The chemical properties of the coke determine the quality of the coke as fuel for the blast furnace to produce heat and as a reductant. Coke contains some undesirable chemical elements such as alkalis (Na_2O and K_2O) and zinc (Zn). The alkalis increase the basicity and increase the volume of the slag. These elements must be kept at a minimum because their presence will raise the furnace fuel rates, (Price et al.1997). The ash content of the coke is of particular concern to furnace operation because higher ash content has a negative affect on the brick life in the furnace (Poveromo, 1997). The CSR (coke strength after reaction) gradually drops as the alkali content increases (Leeder et al 1999).

The American Iron and Steel Institute held a survey in 1995, according to Poveromo (1997) and came up with a set of recommended coal and coke properties as a guideline for blast furnace operation:

Coal:	Stability	> 61 %
	Hardness	> 70 HGI
	Mean Size	> 2"
	Moisture	< 5%
	Ash	< 8.5%
	Sulfur	< 0.75%
	Alkalis	<0.20%

Coke: Coke Strength after Reaction (CSR)	> 61 %
Coke Reactivity Index (CRI)	< 22 %

1.2 Environmental problems related to carbonization and coke utilization

The temperature of the earth's atmosphere is in part regulated by the greenhouse effect. Since the beginning of the industrial era, global warming seems to be increasing. Gases like methane (CH₄), carbon dioxide (CO₂) and nitrogen oxides (NO_x) prevent the escape of the infrared radiation from the earth's atmosphere thus causing global warming. Combustion of coal for power generation and its use in coke making contribute to the formation of the greenhouse gases in a much greater amount than any other industry (Shaw, 1997).

Coal is a complex organic colloid consisting mainly of carbon, hydrogen and oxygen. During the high temperature coke making process, the volatile components are concentrated in the gas phase. If these gases leak into the atmosphere, they contribute to air pollution and in some cases enhance the greenhouse effect.

Different stages in the coke making process are responsible for different types of pollution of the atmosphere and the soil: (Kolijin, 1997).

- a. During the stockpiling, preparation and charging of the fine coal to the coke ovens, dust particles are generated.
- b. Volatile organic carbon compounds (VOC's), carbon monoxide and fine particle emissions leak from the coke ovens during the coke making process, especially if the process is run under a positive pressure.
- c. Fine particle emissions are emitted during the quenching of the hot coke.

- d. Sulfur dioxide, nitrogen oxide and VOC's emissions occur during the combustion of fuel to heat the ovens.

In a by-product coke plant, the types of potential pollution include:

- a. VOC's like benzene, tars and oils may leak into the atmosphere and the soil during the coking process or from the storage facilities.
- b. Ammonia and nitrogen oxides may leak during the ammonia removal from the by-products.
- c. Wastewater contaminated with phenols, cyanide, dioxins and sulfur compounds leaks into the ground water.

Pressure from government agencies and environmentalists to meet stricter environmental standards is responsible for many improvements in the coke making industry, especially, during the last 20 years. Improvements in the design of the door, lid and standpipe sealing systems in conventional coke ovens as well as in the pushing and quenching technologies have been made. Over 6 billion US dollars were spent in the last 20 years in the USA to minimize and control pollutants in the coke industry (Kolijin 1997).

Even with the new laws on environmental control in place by 2003, the conventional coke making technology with by-product recovery plants is still expected to be the main method of coke making in the next decade in the USA. Currently, most of these ovens are more than 30 years old and are nearing the end of their expected lifetime. The coke making and steel industry will have to decide between either new technology coke-making batteries like the beehive type of ovens or alternatively, non-coke methods of steel making.

Beehive ovens operate under a negative pressure. Because of this negative pressure fugitive emission during the coking cycle is remarkably low. Also, because oxygen is

introduced into the oven during the coking process complete combustion of the coal gas takes place and hydrocarbon emissions are almost totally eliminated. This is the biggest advantage of these new technology ovens. This is what is referred to as “non-recovery” technology.

In traditional slot oven technology the coal gas generated during the coking cycle is collected in an elaborate system of piping and collection vessels transporting it to a “by-product” plant where these gases are cleaned and some are recycled to the battery as fuel for the coking process. Volatile compounds driven from the coal are used as fuel to heat the oven.

The U.S. Environmental Protection Agency considers non-recovery coke making to be the best achievable technology under the Federal Clean Air Act, so any new ovens should be of non-recovery design.

Heat recovery ovens represent a new technology in non-recovery beehive ovens in the coke making industry and there is a need for a detailed study of the variation in quality of the coke produced in different sections of a beehive oven.

The samples needed for this study were obtained from a beehive oven at a coke plant in Vansant, Virginia, USA, using coal from USA and Canada. The analytical work was done at the Pearson Coal Petrography lab in Chicago, Illinois. The author of this paper did all the analytical measurements on the samples. Currently, very little literature is available on the behavior of coal and coke in the beehive ovens and no evidence could be found that a similar study to this one has been undertaken before anywhere in the world. Although this study is limited to the northern hemisphere coal it is believed that the results will add value

to all the beehive type coke operations worldwide. It is predicted that future coke plants would move in the direction of beehive ovens instead of slot ovens since it is more cost effective and environmental friendly. This study could be the foundation for others to build on.

2. LITERATURE STUDY

2.1 History of beehive coke ovens

In 1735 Abraham Darby successfully produced iron, using coke. This started the coke era. More and more charcoal was replaced by coke in the blast furnaces and the demand for coke increased. Originally, coke was made by distilling coal in mounds or heaps similar to those used for charcoal making. The growing demand for coke soon resulted in the development of permanent coke ovens. In 1820 the first beehive ovens were built in England. The ovens had a diameter of approximately 3 m (10ft) with a dome height of approximately 2.3 m (7ft). The ovens were frequently built against a hillside in an arrangement of a few ovens together, called a battery. The coal was charged into the oven from the top through an opening in the dome. In the early beehive ovens, some of the coal in the burden and all the by-products were burned and coke yields of between 50 – 60% of the coal charge were obtained (Gray 1997).

The Mitchell ovens were a modification of the beehive ovens and were patented in 1908. The modifications included sole flues to generate heat using the by-product gas. They also had two doors on opposite sides to allow easier discharge and leveling of the coal. The higher dome improved the gas combustion and resulted in more even coking.

The next type of oven in the non-recovery type of coke ovens was the Illawarra oven that was used in the 1920s in Australia. The design also had two doors and the coal could be charged and leveled mechanically and the coke was mechanically discharged. Gas was directed by down-comers to sole flues in the floor where it was burned to allow the coal to be coked from both the top and the bottom of the oven (Gray, 1997).

In the USA, the first beehive oven design was used in the non-recovery Jewell Thompson ovens built in the 1960s in Vansant, Virginia (Figure 1). These ovens were first operated by the Jewell Coke Company, but are now owned by Sun Oil Company. The ovens were modifications of the Illawarra ovens. The modification includes the development of a serpentine sole flue design and operation under negative pressure. These ovens were grouped in four batteries that consisted of 143 ovens each, producing 120,000 tons of coke per year.

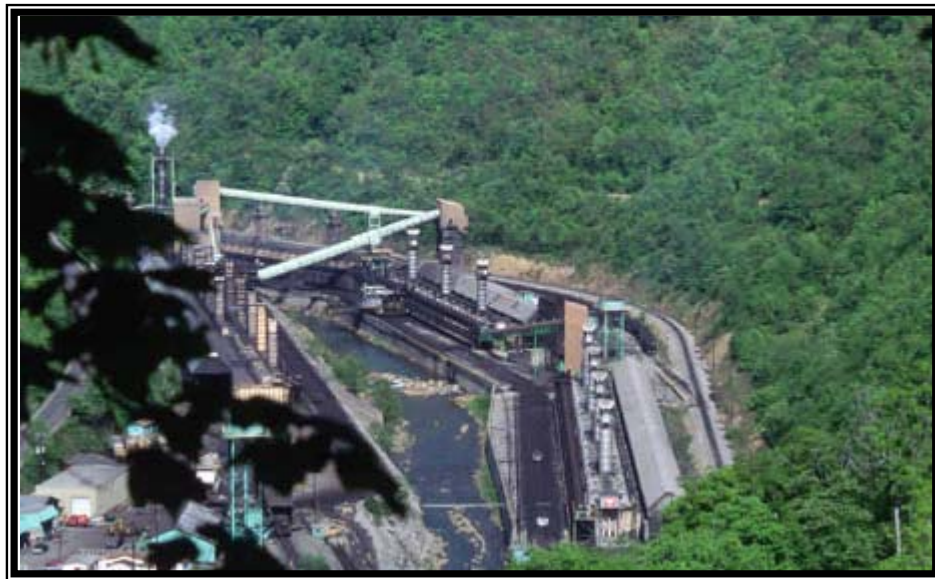


Figure 1: Vansant coke plant in Virginia.

In 1989, a new generation of the Jewell Thompson non-recovery coke ovens (Figure 2) was built at the same Vansant plant. The new ovens were designed to operate within the environmental pollution restrictions of the Clean Air Act Amendment of the USA government of 1990. These ovens produced the highest quality coke in the USA at the time and still remained cost competitive with conventional coke making processes (Ellis and Pruitt, 1999).

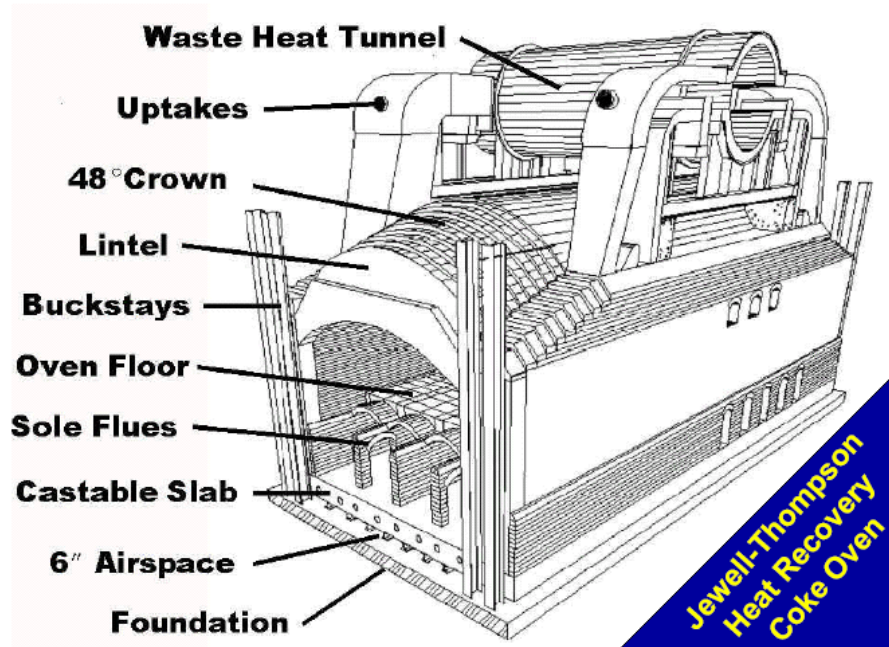


Figure 2: Jewell Thompson Heat Recovery Coke Oven

Other modifications to the Illawarra type have been attempted. The Pennsylvania Coke Technology Inc (PACTI) improved the sole flue design in the 1970s. The PACTI flue system improved the even heating and eliminated the formation of toxic hydrocarbon emissions present in the previous designs. The PACTI design also changed the charging system to improve the bulk density of the coke. While the PACTI process certainly has merit, it is not yet in commercial operation.

Non-recovery ovens run under a negative pressure and by-product ovens run under a positive pressure. Since the gas from the coking process is burned within the oven in the non-recovery plants, it eliminates leakage from doors and ports; a problem that prevails in the by-product ovens. The operating costs of non-recovery ovens are much lower and they can run with cheaper, higher volatile (26%) coal since there is no carbonization pressure as in the positive pressure by-product ovens.

Taking these factors into consideration, the newest and technologically most advanced non-recovery coke plant in the world (Figure 3) was built in 1997 in East Chicago, Indiana as a joint venture between Ispat Inland Steel, Indiana Harbor Coke Company and Primary Energy. It consists of 268 ovens grouped in four batteries. It produces 1.2 million tons of coke per year. The waste heat from gas generates steam that in turn generates 87 MW of electricity (Ellis et al., 1999). (Figure 4).



Figure 3: Indiana Harbor Coke Plant on the shores of Lake Michigan in Gary IN.

Recovering Waste Heat- Flue Gas Flow Diagram

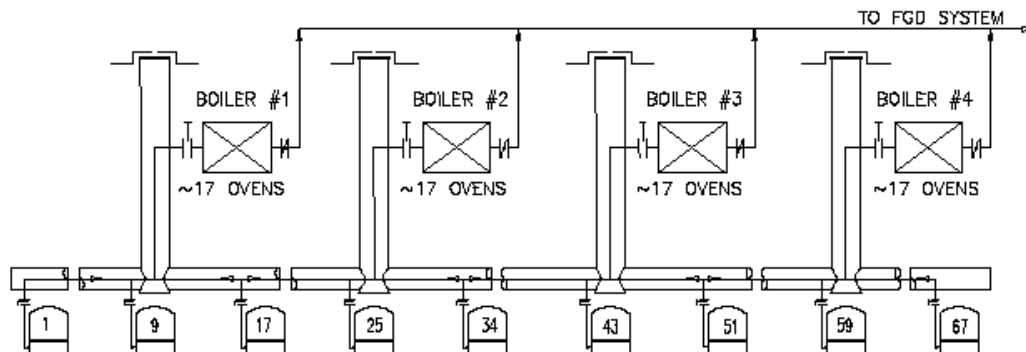


Figure 4: The waste heat used for steam production to generate 87 MW of electricity.

2.2 Operation of beehive ovens

The coal is loaded into the beehive oven by removing its front door, or sometimes through a loading opening on the top of the oven. The refractory bricks maintain the heat of the previous coking cycle and initiate the degassing of the newly charged coal. The required heat for the coking is supplied by partial combustion of the coal.

The gas generated by the coking cycle exits the oven through ports in the wall and flow into down-comer pipes to the floor of the oven. The hot gas helps to heat the coal on the floor so that the coking process can occur simultaneously from the top of the coal bed downward and from the bottom upward. The gas from each battery of ovens is tunneled to the waste heat boilers. From there it is transported to a nearby energy company that uses it to produce electricity.

The coking cycle takes between 42 and 48 hours. Then the front door is removed and the coke is pushed onto a coke guide or hot car and taken to the quenching stations.

2.3 Plastic zone and gas flow

According to the carbonization research of Van Krevelen and co workers (Van Krevelen, 1961), the carbonization process from coal to coke can be viewed as taking place in stages. The heat is transferred from the heated brick walls of the coke oven into the coal charge and the first stage of coke making takes place from 90 – 150 °C when mainly moisture is removed from the coal.

The second stage is the primary devolatilization stage. The coal softens and volatiles are released. This occurs between 350 – 550 °C when the chemical decomposition takes place, and an intermediate phase, called the metaplast is formed, which is responsible for the plastic behavior of coal. During this stage, the plastic layers are formed near each wall. At the end of this stage, which is characterized by mainly endothermic reactions, an exothermic reaction takes place, which is caused by the re-solidification of the plastic mass at about 500 °C.

Next is the shrinkage and cracking stage in which tar is vaporized and non-aromatic groups are split off. Re-condensation and formation of semi-coke takes place at 670 – 720 °C. The last stage is characterized by the degasification reactions in which the semi-coke units are welded together by evolution of methane and hydrogen to yield the final coke.

To get a better understanding of the coking conditions in a non-recovery coke oven, a thermographic profile was drawn up from data gathered by infrared imaging and video

imaging. The temperature was measured at intervals during carbonization and a temperature profile was constructed for the whole coke cycle. The temperature peak was reached at 42 hours after the coal was loaded and it represented the time when the two plastic zones, originating from the top and bottom of the bed met in the middle (Gray, 1997).

Between the softening coal and the semi-coke a small gap of about a millimeter wide was present. Fissures formed in the coke mass from the cauliflower end to the hot surface of the plastic layer. The fissuring is influenced by the heating rate and temperature. Therefore, fissures are more significant near the heating element (Rhode, 1997).

Gas was generated in the decomposing, softening coal mass, but the coal mass had a low permeability. In the gap in the plastic zone, the pressure built up since both sides of the plastic layer had low gas permeability. This is one of the reasons for wall pressure and the formation of sticker charges in the slot ovens (Rhode, 1999).

In an experiment in which fine gas probes were integrated into the charge, it was found that shorter distances to a fissure line were directly related to lower gas pressures (Rhode, 1999). The conclusion is, therefore, that the gas that built up in the plastic zone flowed through fissures in the coke mass, but could not move through the plastic zone.

After experimenting with gas probes at a non-recovery coke oven, it was found that about 90% of the raw gas that formed in the plastic zone moved through the coke mass towards the sides of the oven while the remaining 10% of the gas flowed into the non-carbonized charge (coal). The raw gas that flowed through the fissures was responsible for the deposition of pyrolytic carbon (Arendt, et al., 1999).

2.4 The future of coke ovens in the USA

Effects of the Clean Air Act of 1990 redirected the attention of North American coke makers to non-recovery coke making technology. The maintenance is significantly less than on the tall by-product ovens; furthermore, there are no complex by-product plants, and a wider range of coals can be used. There is no emphasis on coking pressure since the non-recovery plant operates under negative pressure. Furthermore, by-product ovens have a low profit margin. Therefore all new coke ovens that will be built in the future in the USA will probably be beehive type (Walters, 1999).

3. PROBLEM STATEMENT

Currently, very little is known about the quality variation of coke formed in the non-recovery ovens. This project aims to model the behavior of the coal-to-coke process and predict the areas in the oven where the highest quality coke is formed. This might enable coke makers to produce different quality coke products for different markets.

Problem statement background

The current criteria for measuring the quality of coke are based on physical properties, chemical properties and metallurgical performance. The physical properties include stability, hardness, size grading, porosity and moisture. The chemical properties are ash, sulfur, volatile matter and alkali contents and the metallurgical properties are CSR and CRI indexes (Keagi, 1981). As long as these values, determined on relatively small samples, are within specified upper and lower limits, the whole charge of coke will be acceptable for use in the blast furnace, although it is known that the quality of coke differs from place to place within the oven.

One critical criterion for measuring coke quality is CSR. CSR describes the coke strength after reaction in the furnace. Many blast furnaces require values between 50 and 60 and even in the higher 60s for the larger furnaces. Higher CSR numbers are generally preferred.

Higher CSR coke exhibits higher levels of pyrolytic carbon content than lower CSR coke. As the coal is progressively converted into coke, the first formed coke is exposed to raw gas from coal that is still being carbonized. CSR should improve during the coking because the coal gas condenses into the open fissures in this early converted coke. In the non-recovery ovens, the coal gas flow is moving through the top layers of the coke, which results in the deposition of pyrolytic carbon in coke. Therefore it is expected that the highest CSR should occur in the top layers of the coke bed and the lowest CSR on the bottom of the oven.

In heat recovery as well as slot ovens, coke quality differs because of the flow of gas through the coke during the coking cycle. For slot ovens, more than 90% of the gas passes through the coke along the walls of the coke oven, thus the highest quality coke is along the sides of the oven. Gas from the heat recovery ovens is partly combusted within the oven. Most of the gas passes through the top layer and the sides of the coke bed. Air from combustion is introduced via ports in the oven doors. The amount of air is controlled to maintain the desired temperature in the oven. The rest of the gas exit through passages in the oven walls and enter into the sole flues. There final combustion takes place resulting in exhaust gas. Emission of toxic chemicals is largely prevented since the oven operates under negative pressure in a controlled oxidizing atmosphere. Some of the tar and light end gas generated during the early part of the coking cycle condenses and carbon is deposited within the fissures of the coke during the coking process. This accounts for the higher variability of the CSR in the coke bed and other coke qualities within the oven.

In order to produce the highest quality coke for the least money and least pollution, an understanding of the variability of coke quality within the coke oven is needed. Porosity, coke strength after reaction (CSR) and coke reactivity index (CRI) all vary with distance from the heat source in the oven.

Extensive studies have been done on these criteria in the traditional slot ovens but little has been published on heat recovery ovens. In previous studies, it has been found that the quality of coke in the conventional slot coke ovens depends on where in the coke oven the sample has been taken (Arendt et al., 1999).

4. EXPERIMENTAL METHODS

4.1 Sampling

The sampling took place at the Vansant Plant of the Sun Coke Company in Vansant, Virginia, USA, which uses the new generation of Jewell Thompson non-recovery coke ovens similar to the ovens used in the Indiana Harbor Coke plant in Gary, Indiana.

The sampling strategy was to obtain a whole block of coke exactly as it was positioned in the oven so that individual samples from different parts of the oven could be compared with each other to investigate the spatial variation of coke quality parameters in the heat recovery and by-product coke ovens.

An oven from the middle of Battery F was chosen for the test. After the coking process, half of the oven was pushed out onto a hot car and taken to the quenching station. The

remainder of the coke in the oven was carefully pushed out onto a coke guide car so that it remained in one block exactly as it was in the oven (Figure 5). The block of coke, approximately 3.6 m (12ft) wide, 1 m (38 inches) high, and 2.7 m (9 ft) long remained on the coke guide. The approximate mass of the block of coke was 5500 kg (12,000 pounds). The coke guide with the coke was moved to a secure location and hand quenched with water. After the coke had cooled overnight, a series of photographs were taken so that the exact position of each sample could be recorded.



Scale: 10mm = app 1m

Figure 5: Coke guide with massive sample as retracted from the oven.

Coke from the top of the bed was sampled and marked as “T” (top), that from the sides of the bed was marked as “S” (side), and that from the bottom was marked as “B” (bottom) (Figures 6-9). Enough coke was taken from the same area to perform all the required tests on it so that a full set of results would be available for each section.

A representative sample of the coal charged into the oven was taken for petrographic analysis. The charge coal consisted of a blend of five Virginia coals.

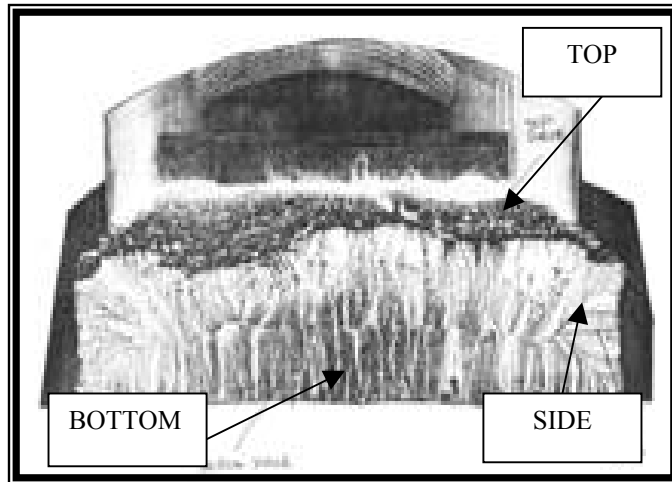
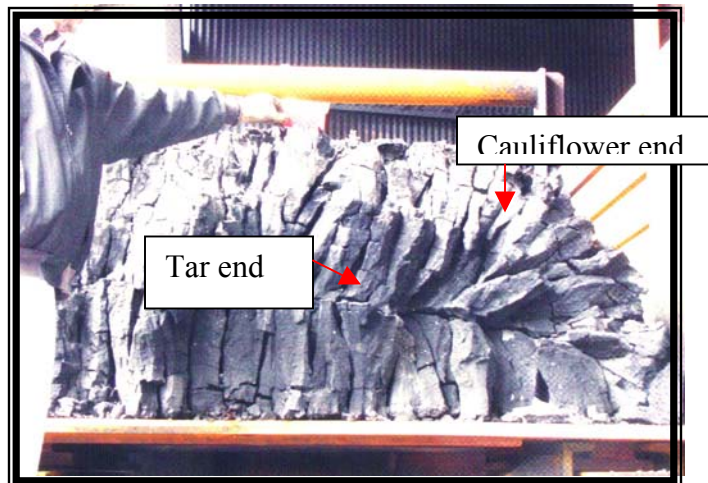


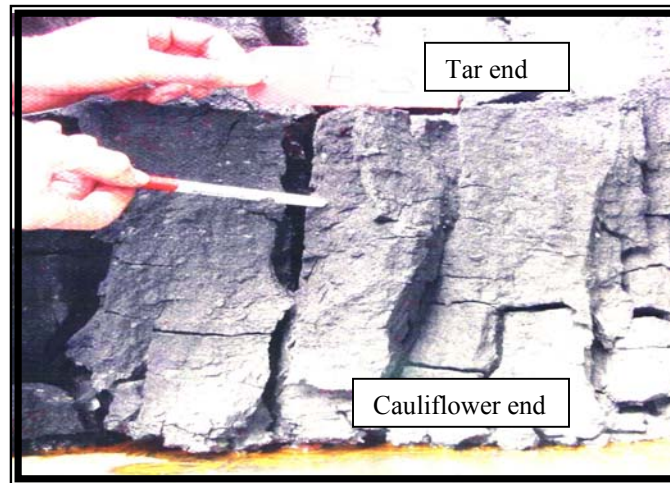
Figure 6: The coke taken from the top of the coke bed was marked T, from the side, S and from the bottom B.



Scale: 1mm = app. 2 cm

Figure 7: Appearance of coke piece T from the top of the coke bed.

The coke closest to the heating zones is called the cauliflower end and the part in the middle of the coke bed is called the tar end. The cauliflower end has got characteristic swelling patterns that resemble a cauliflower head.



Scale: 2mm = app. 1 cm

Figure 8: Close up of coke piece B from the bottom of the coke bed.



Scale: 1mm = app. 2 cm

Figure 9: Appearance of coke piece S from the side of the coke bed.

4.2 Sample preparation for petrography

The three pieces of coke marked, T, B and S for petrographic analysis were taken as shown in Figure 6. Each piece was divided into three zones, the cauliflower zone, middle zone and the tar zone, based on visual differences in structure (Figure 10).

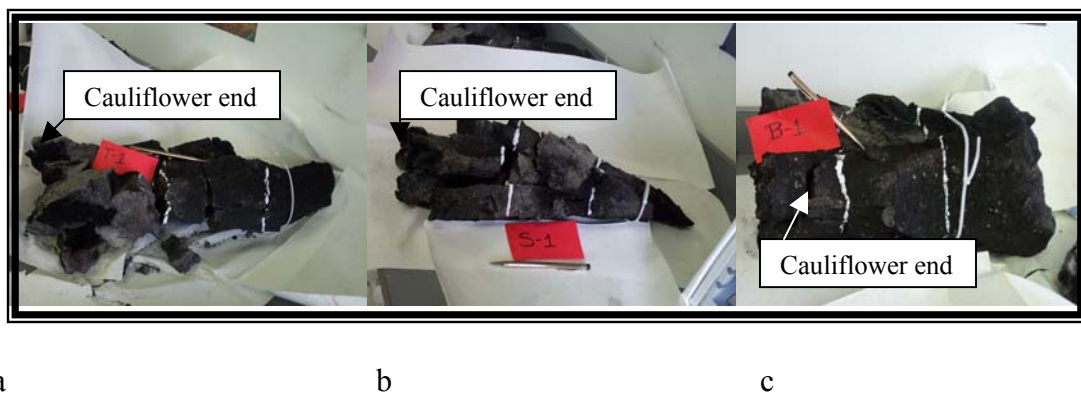


Figure 10: (a) Coke piece “T” from the top of the coke bed; 20” (app. 51cm) long,

(b) Coke piece “S” from the side of the coke bed; 19.25” (app. 49cm) long,

(c) Coke piece “B” from the bottom of the coke bed; 12” (app. 31 cm) long.

Each piece was then cut up into layers, starting at the cauliflower end; each layer was identified with an alpha character, layer A being the first layer. Each layer was about 2” thick (Figure 11).

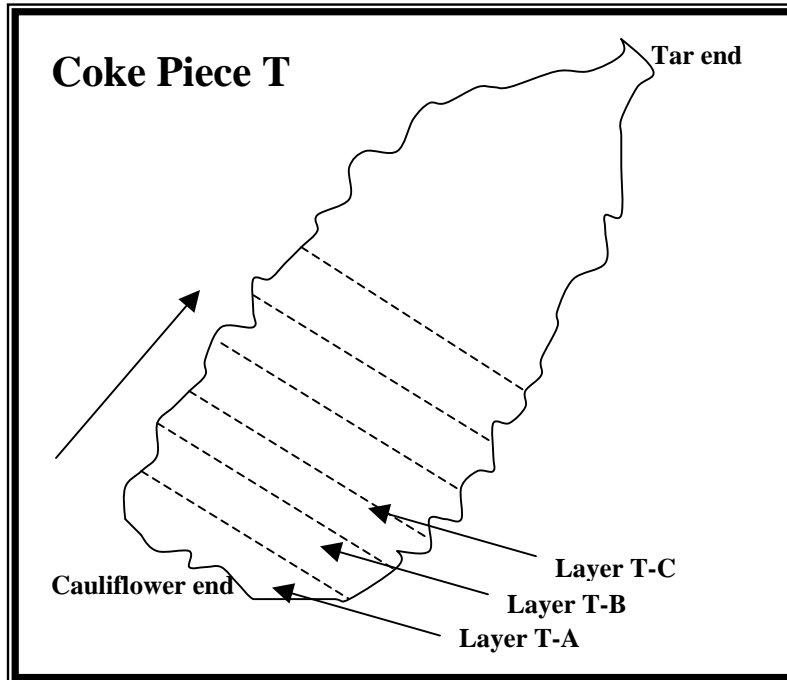


Figure 11: Schematic plan for cutting up large coke pieces into layers, starting at the cauliflower end and using the labels with alpha characters, starting at layer A.

The layers were then returned to their original position, and each layer was cut into individual pieces that will be referred to in the rest of this report, as “samples”. The first sample, on the left back corner of each layer was numbered 1, the sample next to it, number 2. The sample in front of sample 1 was numbered 1-1 and the sample in front of it was numbered as 1-2. The sample in front of sample 2 was numbered 2-1 and 2-2 and so on (Figure 12). Coke piece T was cut into 110 individual samples, coke piece S into 73 samples and coke piece B into 79 samples.

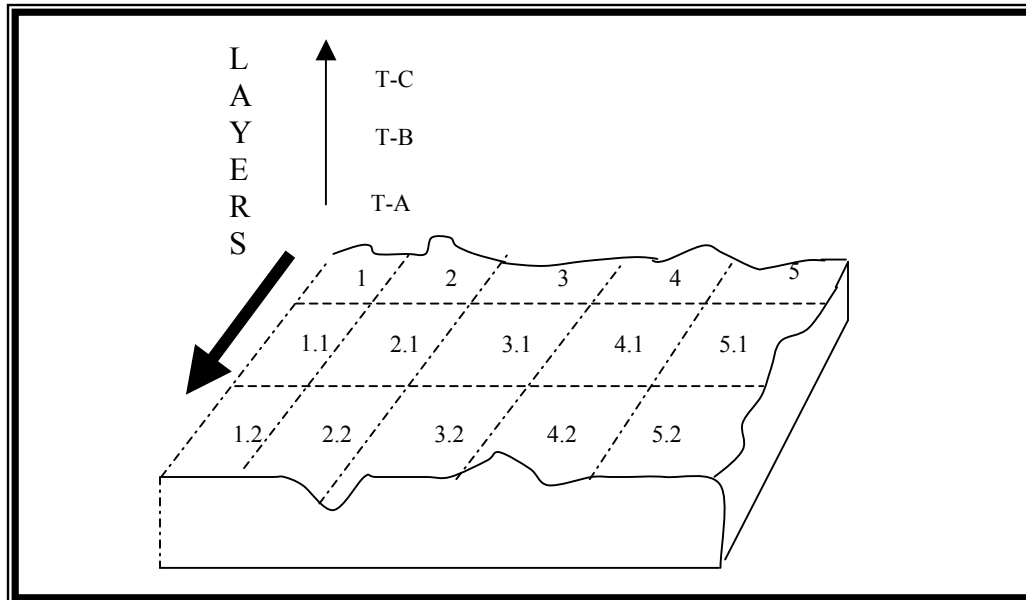


Figure 12: A schematic plan to cut each layer into individual samples. Starting in the back left corner, the first sample was labeled as 1; the one in front of it is labeled as 1.2 and the one to the right of it the number 2.

The following Table 1 shows the number of layers and samples in each coke piece. The average number of samples per layer is not constant due to the irregular shape of each coke piece.

Table 1: Sample distribution

Piece	Layers	Samples	Average number of samples per layer
T (Top Piece)	15 layers T-A to T-O	110	7
S (Side Piece)	13 layers S-A to S-M	73	6
B (Bottom Piece)	9 layers B-A to B-I	79	8

4.3 Analysis on coal

The coal blend was made up of coal from different mines in Virginia, USA. The coal was submitted to various analyses. The analysis is described below and the results are given in Table 4 on page 27.

4.3.1 Volatile matter (ASTM number D3175) and moisture (ASTM D3173)

Coal passing through a 212- μm sieve is heated for 7min at 900 °C out of contact with air. The volatile matter content is calculated from the loss in mass of the sample less the loss in mass due to the moisture content. The moisture content of the sample must be determined at the same time as the volatile matter content.

For the moisture content of the sample, 1.0g of the sample is loaded into a heating capsule and placed for one hour in an oven that has been pre-heated to 110 °C. The capsule is then taken out of the oven and left to cool before it is weighed again. The moisture of the sample is calculated according to the following formula:

Moisture of sample = $[(A-B)/A] \times 100$

Where: A = mass of sample used (before heating) and

B = mass of sample after heating

The result of this test is used to calculate other relevant analytical results to a dry basis. (ASTM, 1996)

For both the volatile matter and moisture tests, it is essential to carefully regulate and monitor the rate of heating, final temperature and overall duration of the test.

The volatile matter content is calculated according to the following formula:

$$V_m = \frac{100 - (m_1 - m_2)}{m_1 - m_2} - M$$

Where: m_1 = initial mass of crucible plus sample

m_2 = mass of crucible plus residue of sample after heating

M = moisture content

4.3.2 Ash (ASTM number D3174 or D5142)

This test is to determine the inorganic residue left as ash from the coal or coke sample after burning. The sample is crushed to pass through a 250- μ m sieve. One gram of the sample is loaded into a cold capsule and placed in a cold oven. The oven is heated at a rate to reach 500°C in 1 hour. It is then heated further at a slower rate to reach 750°C after the

second hour. The oven temperature is kept stable for another two hours between 700°C and 750°C. The capsule is removed from the oven to cool and weighed again as soon as it reaches room temperature. The ash content of the sample is calculated according to the following formula:

$$\text{Ash in sample} = [(A - B)/C] \times 100$$

Where A = mass of the capsule, cover and ash residue

B = mass of empty capsule and cover and

C = mass of analysis sample used.

Ash is the inorganic residue remaining after burning the coal and/or coke. The mass of the ash differs from the mass of the inorganic constituents present in the original coal due to chemical reactions during the heating process, and generally is about 80 to 90% of the mass of the inorganic material matter in coal. (ASTM, 1996).

4.3.3 Fixed carbon

The fixed carbon is not a physical test, but a calculation using the moisture content, the ash content and the volatile matter of the coal.

The fixed carbon is calculated with the following formula:

$$\text{Fixed carbon \%} = 100 - (\% \text{ moisture} + \% \text{ ash} + \% \text{ volatile matter})$$

4.3.4 Sulfur (ASTM number D4239)

There are three alternatives to this test procedure. All the alternatives involve high temperature combustion but with different sulfur detection procedures in one of the methods. The sample is crushed to pass through a 250- μm sieve; 0.5 gram of the sample is spread out evenly in a combustion boat, which is placed halfway inside the tube of the oven and left for a few minutes to drive off the volatiles. The boat is then moved further into the oven and left for about 15 minutes at 900 °C. The combustion gas leaves the tube through the exit end and is dissolved in hydrogen peroxide and titrated with sodium hydroxide. The sulfur is calculated from the burette reading during the titration process (volume), and is part of the ultimate analysis of coal. The results can be used to evaluate the coal in terms of sulfur emission from the coal combustion and quality in relation to contract specification. The test provides a rapid and reliable method to determine the sulfur content in a sample. (ASTM, 1996).

4.3.5 Calorific value (ASTM number D5865)

This procedure is used to determine the heat of combustion or calorific value of coal that is burned as fuel by using either an isoperibol or adiabatic bomb calorimeter. The calorific value is defined as the quantity of heat that can be liberated from one pound of coal measured in BTU's. (B.T.U. – British thermal unit: The amount of heat needed to raise one pound (454g) of water one degree Fahrenheit). To determine the calorific value, coal is crushed to pass through a 250- μm sieve. About 1 g of the sample is weighed and put in the bomb part of the calorimeter. The flow of oxygen to the bomb is opened. The calorimeter vessel is filled with water at room temperature around the bomb. The temperature is checked to ensure that the temperature remains stable. The charge is fired to ignite the sample and the rise in temperature of the water is recorded. Gross calorific value is calculated using the rise in temperature of the water and correction factors are used for acid used in the ignition process, for sulfur in the coal and the mass of the sample.

4.3.6 Alkalis (ASTM number D3682)

This test is used to determine the common major and minor elements in coal ash and coke ash. The ash sample is ground to pass a 74- μm sieve. The sample is reignited at 750°C for one hour and rapidly cooled and weighed out for analysis. An ash sample of 0.1 g is mixed with lithium tetraborate and placed in a pre-heated furnace at 1000°C to fuse. When the sample is cooled, it is mixed with HCl and boiled for 30 minutes. The solution is cooled and used to determine the SiO_2 , Al_2O_3 , Fe_2O_3 , CaO, MgO, Na_2O , K_2O and TiO_2 by titration. The result of these tests is useful for the total description of the quality of the coal. It is also helpful to predict the behavior of the ash and slag formed during combustion in the coke oven (ASTM, 1996).

4.3.7 Free swelling index (FSI) (ASTM number D720)

One gram of –60 mesh coal is rapidly heated to 820 °C in a porcelain crucible. The crucible standard is 41 mm in diameter and 26mm in height. The coal normally swells to form a button that is characterized by comparing it to a set of standard profiles. The more the coal swelled and the higher the button is, the higher is the FSI. The FSI can vary between 1 and 9. If the FSI is over four, the coal is classified to have moderate coking properties and if the FSI is over six and a half, it is considered to have high quality coking properties (Price et al., 1997 & ASTM, 1996).

4.3.8 Gieseler plasticity test (ASTM number D2639-90)

The Gieseler plasticity test measures the degree of softening as well as the swelling, plasticity and re-solidification temperatures of the coal. A good coking coal must be able to melt partially so that it can bind the solid particles together. Coal with a low plasticity can be blended with coal with a high plasticity to improve the coking properties of the blend.

In this test the coal is heated at a constant rate while being stirred. The crucible with stirrer and sample to be tested are immersed into a bath to provide temperature uniformity. The starting temperature is usually 380°C and the standard stirrer is loaded by a constant torque of 101,6 g/cm. Revolution of the stirrer is observed while the heating rate of 3 °C per minute is applied. The velocity of revolution and current temperature are noted and recorded to provide mathematical and graphical processing.

When the coal becomes plastic, the stirring rate increases until it reaches a maximum speed of the stirring arm. As the coal re-solidifies, the movement slows down until the stirring arm of the plastometer comes to a complete stop. The rotations per minute are registered on a dial. The softening temperature is registered when 0.5 dial divisions per minute (ddpm.) is reached. Maximum fluidity temperature is registered when the maximum speed of the stirrer arm is reached. Solidification temperature is registered when the stirring arm comes to a complete stop.

Results of the tests are used for determining a plastometric index of coal and its mixtures used in coke production (ASTM, 1996).

4.3.9 Hardgrove grindability (ASTM number D409)

This test is done to determine the relative grindability or ease of pulverization of a coal compared to a chosen coal standard. A dry sample is crushed and sieved to prepare it for the test. A sample of 50 g of size portion of 500µm to 1000µm (16 to 30 mesh) is used for the test. The sample and iron grinding balls are placed in the Hardgrove grindability machine and tumbled for 60 revolutions. The grinding balls are gently brushed off and removed from the coal sample. The coal dust is then sieved for 10 minutes in a mechanical sieving machine using a 75µm (200 mesh) sieve. The material left on the 75µm sieve and

the material that went through the 75 μ m sieve is weighed separately. The Hardgrove Index, HGI is then calculated using four standard values and a formula that is calculated from a standard Hardgrove graph. The result is given as a SI unit called the Hardgrove Grindability index (HGI). The results of the test can be use to evaluate the yield or energy input, or both, required in a grinding or pulverizing process (ASTM, 1996).

4.3.10 Size analysis (ASTM number D293)

This test method is to separate a coal or coke sample into defined size fractions. The material must be dry. The results of this test were not available to include in the report. Sieves are stacked from the one with the largest openings at the top to the one with the smallest openings at the bottom. The sieves are shaken vigorously to allow the sample particles smaller than the sieve openings to fall through to the next sieve with the smaller openings. After a specific period of time, the material left on each sieve is weighed and expressed as a percentage of the gross sample for each sieve fraction. (ASTM, 1996)

4.3.11 Ash fusion temperature (ASTM number D1857)

The ash fusion temperature is determined according to the ASTM D1857. A small pyramid is pressed from coal ash. The pyramid is placed in a furnace and heated in a mildly reducing or oxidizing atmosphere. The temperature range generally used is 900°C up to 1600°C, and the temperatures which can be recorded are the initial temperature, the deformation temperature, the softening temperature, the hemisphere temperature and the fluid (flow) temperature. The deformation temperature is recorded when the top point of the pyramid becomes rounded. The softening temperature is taken when the pyramid is about two-thirds of its original height. The hemisphere temperature is when the pyramid has melted so much that it looks like an upside down half of an orange at half the original height of the pyramid; and the flow temperature is when the pyramid is completely melted

(ASTM, 1996). For the purpose of this report, the ash fusion temperature was determined in a USA lab and is given in °F in Table 4.

4.3.12 Coal rank (ASTM D2798 and ISO 7404-5-92)

The petrographic analysis of the coal includes the determination of rank as well as the maceral composition and is a major tool for predicting coke strength. Both tests are done on the same sample so the sample preparation for both tests are the same. Coal is crushed to pass through a 20-mesh sieve. It is then mixed with a resin and allowed to set in a (typically) 25 mm diameter cylindrical briquette. The briquette is then ground and polished.

The mean maximum reflectance of vitrinite in coal is an indication of rank or the degree of metamorphism the coal has undergone. It is measured under the microscope by focusing on vitrinite and rotating the polished sample 360 ° through a polarized light source. The amount of light reflected from the vitrinite is measured very precisely using a photometer mounted on a reflecting light microscope. The reflectance can vary between 0.4% for high volatile bituminous coals to more than 2.0% for anthracite. The mean maximum reflectance value is calculated from at least 100 readings. Each reading is classified into a V-class. For instance, all the readings of light reflectance between 0.50% and 0.59% would fall into class V5, all readings between 0.60% and 0.69% into class V6 and so on. Only vitrinite in classes V5 to V18 is capable of becoming plastic in the coke (Greeff, 1988).

Various parameters of the coal, for instance the volatile matter, equilibrium moisture and fixed carbon content are determined by the rank and maceral composition of the coal. In the coking process, the coke, gas, tar and light oil yields are all related to the rank of the

original coal. The higher the rank of the coal, the higher the coke yield and the lower the yield of gas and light tars are during the coking process (Price et al., 1997).

4.3.13 Maceral Analysis (ASTM2799 and ISO 7404-3)

The maceral analysis is done by counting at least 1000 points by means of a mechanical stage attached to the microscope stage. These maceral groups are identified as vitrinite, liptinite and inertinite. Each group includes a series of macerals. The vitrinite group includes telinite, collinite and vitrodetrinite. The exinite group includes sporinite, cutinite, alginite, resinite and liptodetrinite. Lastly, the inert group includes fusinite, semifusinite, secretinite, micrinite, macrinite and inertodetrinite (Falcon and Snyman 1986).

The macerals can also be grouped into the reactives, semi-reactives and inerts according to their behavior during carbonization. The reactive group includes the vitrinite and exinite groups. The semi-fusinite makes up the semi-reactive group and the inert group includes the macerals of the inert group (Valia 1997).

The mineral matter is calculated from the ash and sulfur contents (Price et al., 1997).

$$\textit{Mineral matter} = 1.08 \times \textit{ash} + 0.55 \times \textit{sulfur}$$

4.3.14 Composition balance index

The composition balance index is the relation between the total amount of inerts and the amount of inerts needed for optimum coke strength. The optimum amount of inerts is calculated from the V-type data by allocating the optimum of inerts to each V-class. The sum of these optimum amounts inerts for each V-class is the optimum inerts of the coal.

The composition balance index is then calculated by means of the following formula (Greeff, 1988)

$$\textit{Composition balance index} = \frac{\textit{total inerts in coal}}{\textit{optimum inerts in coal}}$$

4.4 Analysis on coke

4.4.1 Coke reactivity index (CRI) and coke strength after reaction (CSR) (ASTM D5341)

These tests are patterned after the Nippon Steel tests. A dried coke sample is reacted with CO₂ gas at elevated temperature (1100 °C) for a specified length of time. The coke reactivity index (CRI) and the coke strength after reaction (CSR) is both determined using the reacted coke residue. The weight loss in the sample after the reaction determines the CRI. The weight retained after sieving and tumbling the reacted coke determines the CSR.

After the sample cooled down, it is weighed.

The CRI is calculated with the following formula:

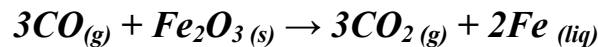
$$\textit{CRI} = (A - B) / A \times 100$$

Where:

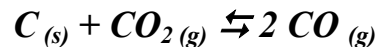
A = original test sample mass prior to reaction and

B = sample mass after the reaction in CO_2

The result of the test is useful to predict the chemical reaction of the coke lumps with the CO_2 gas when it is heated in the blast furnace. In the blast furnace iron ore is reduced by carbon monoxide formed by combustion of the coke in a controlled oxygen-poor atmosphere:



The CRI is an indication of the equilibrium in the reaction



The CSR test is used to determine the strength of lump coke after the CRI test has been done by tumbling it in a cylindrical chamber called an I-tester for 600 revolutions in 30 minutes. It is then sieved, using a 9.5 mm sieve. The fraction remaining on the 9.5 mm sieve and the fraction passing through the sieve are both weighed.

The CSR is then calculated by means of the following formula:

$$\text{CSR} = C / B \times 100$$

Where:

B = sample mass after the reaction in CO_2 and

C = sample mass of the +9.5mm material after tumbling.

The coke strength after reaction is useful to predict the break up of the coke particles in the blast furnace as they rub against each other and against the walls of the furnace to break up and form fine material (ASTM, 1996).

4.4.2 Sample preparation for microscopical analysis

Each sample was chipped to fit inside a 3.8 cm (1.5”) round, plastic sample holder. The sample holder was filled with white epoxy resin and allowed to dry for 24 hours. The white colouring was used to increase the contrast between the resin and the coke for easier identification under the microscope. The dried samples were taken out of the sample holders, and slowly and carefully cut (100 rpm) with a Buehler Isomet 1000 diamond saw to expose the coke surface and to prevent ripping out of the cell walls.

After cleaning in an ultrasonic bath, the cut sample was dried and impregnated with white resin in a Buehler vacuum chamber. Inside the chamber a table that can be rotated from the outside by means of a hand-held switch is connected to a vacuum pump equipped with a barometer.

A piece of masking tape was wrapped around each sample to form a cup to hold the resin on the top surface of the cut sample. The resin was prepared according to manufacturer’s instructions and the paper cup with the resin placed in the centre of the chamber. After the air was removed from the chamber (and the pores of the coke), the cup with the resin was slowly tipped over to allow the resin to run out into the sample. By rotating the stage, all the samples could be filled with resin and air was allowed back into the chamber to reach atmospheric pressure. The samples were removed from the chamber, the tape removed and the sample tipped over on a clean sheet of plastic in order to drain excess resin and allowed to dry for 24 hours. The samples were then ready to be polished.

The polishing was done by means of a Buehler Ecomet 2 polisher, which takes six samples into one sample holder. The following procedures in Tables 2 and 3 were followed for the grinding and polishing of the coke samples:

Table 2: Grinding parameters

Step	Pressure (kg/cm ²)	RPM	Minutes	Fluids
Initial grinding 75- μ m diamond disk	10	120	1	H ₂ O
Final grinding 15 μ m diamond disk	10	120	2	H ₂ O

After the initial grinding of one minute, the samples were inspected. More often than not, only one or two samples in the sample holder were ready for the next stage while the rest of the samples needed more grinding. The samples were ready for the final grind when the layer of resin was ground off to expose the black coke surface and the white resin within the pores of the coke. If the top layer of resin has not been ground off after one minute, it was ground for longer, but had to be inspected about every 15 seconds. If the samples were ground too long, the pores would be open and the sample would have to be impregnated again to prevent breakage of the pore walls during the grinding and polishing of the samples.

Table 3: Polishing parameters

Step	Pressure (kg/cm ²)	RPM	Minutes	Fluids
Polish Texmet cloth, 0.3 μ m γ -Al ₂ O ₃	10	120	6	last 20 seconds using H ₂ O only

The samples were polished for 6 minutes, inspected and polished longer if necessary. After a smooth, shiny surface had been obtained, the samples were taken out of the sample holder, dried with hot air and stored in a desiccator, ready for the microscopical analysis.

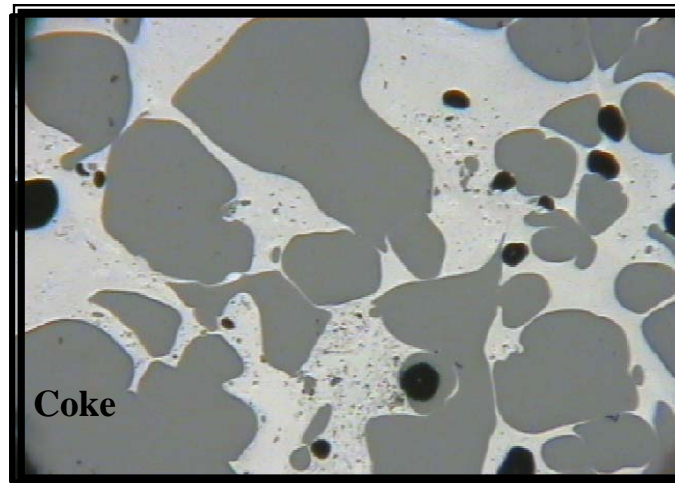
4.4.3 Structure (Image analysis)

Each sample is scanned by means of an automated image analyzer to determine the cell wall thickness and pore diameter. The sample is leveled on a metal plate with a piece of modeling clay before it is placed on the microscope stage. For this analysis, an 8x objective is used. The microscope is connected to a computer and equipped with an automated stage with two stepper motors and a 512 X 512 CCD Camera (Figure 13).



Figure 13: Microscope and computer set up with automatic stage and stepper motors for scanning the coke.

The program used to scan the coke was custom-developed by Pearson Coal Petrography Inc. The program measures the porosity, cell wall thickness and pore diameter of the coke. Figure 14 shows an image of coke under the microscope. The coke, normally black in a hand specimen, show up as whitish grey under the microscope. The pores that are filled with white coloured resin shows up as dark grey to black under the microscope.



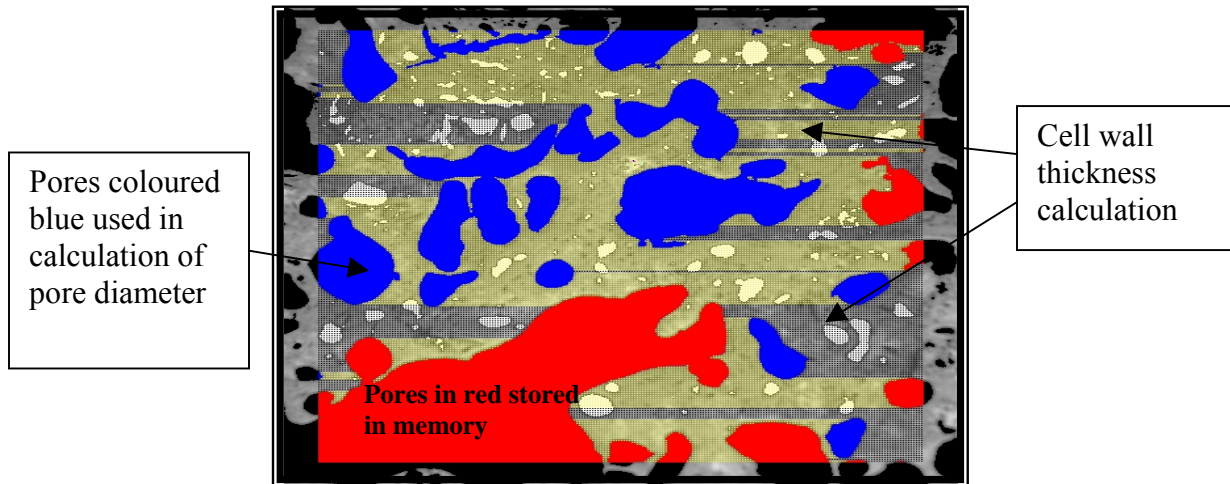
50x magnification

Figure 14: Microscope image of coke. Pores dark grey to black and coke cell walls white.

The image of the coke as seen on the computer screen is shown in Figure 15. The cell wall thickness is measured by the yellow and grey horizontal lines. The yellow lines represent the cell wall thickness of the coke that are completed in the current image on the screen, and the grey lines represent cell walls that would carry on in the adjacent microscope fields (outside the current view). The grey lines are kept in memory and are only added to the calculations when it is completed in the next field of vision.

The same principle is applied to the pore diameter analysis. The pores are coloured red and blue. The blue coloured pores are the pores that are completed in the present field and are used as such in the calculation of the pore diameter. The red colored pores are open-ended

and are completed in the adjacent microscope fields. Since the program is written in such a way that the field next to the one in Figure 15 will also be measured as the microscope stage is moved on, the pores in red will be stored in the memory and will be completed in the next field when the measurement is completed.



50x magnification

Figure 15: Image on the computer screen during scanning of the coke structure. Blue and red colours represent the pores. The yellow and grey lines represent the measurement of the cell wall thickness.

A pre-set cut-off of grey scale values in the program permits distinguishing between the coke and the resin. The cell wall thickness of the coke (white and lighter shades of grey) and the diameter of the pores (dark grey and black) are measured in vertical and horizontal directions.

When the measurements of one field are finished, the automated stage moves on in the X-direction to the next frame. Each frame size is 1175 by 1175 μm (1.175 by 1.175 millimeters). A single frame has up to 262 144 valid data points. The automatic stage only

moves in the X-direction and the operator must prompt the movement in the Y-direction after completion of a row of frames in the X-direction. The program will disregard any frames containing more than 90% resin or pores.

After 100 fields have been measured, the computer automatically calculates a mean value for the pore diameter and cell wall thickness for the whole sample. From these two properties the porosity is calculated according to the following formula:

$$(total\ pore\ data\ points) / (total\ valid\ data\ points) \times 100 = total\ porosity\%$$

The end result, as well as a picture file of each frame, is stored in the memory.

4.4.4 Texture (Point count analysis)

The maceral group vitrinite forms vitrinoké when it is heated under coke-making conditions. The vitrinoké is isotropic when the reflectance of the vitrinite is <0.8%. If the rank of the original vitrinite was >0.8%, anisotropic vitrinoké types form. Firstly, a fine mosaic forms with crystals of about 0.5- μm . As the rank of the vitrinite increases, medium mosaic (crystals 0.5 – 01.3- μm), coarse mosaic (1.3 – 5- μm), lenticular (5-10- μm) and ribbon (>10- μm wide) structures are formed.

In the lenticular and ribbon structure, all the crystals are orientated in the same direction. In the ribbon structure, the individual crystals have flowed together to form one larger structure that resembles a ribbon.

The macerals of the inert group form inertinoké after carbonization. It is divided into isotropic and anisotropic forms, based on the optical properties, including the change of color if the plane of polarizing is changed.

The texture analysis comprises the point counting of individual carbon phases. Since the carbon phases result from the type and rank of coal, it can be expected that the texture of the coke should remain basically the same throughout the whole oven charge, since the coal that was loaded into the oven is a homogeneous blend of different coals. The only expected change is the amount of pyrolytic carbon. The different textures of the vitrinite and inertinite were determined by means of counting 1000 points using a semi-automated stage and a point counter.

5. RESULTS

The results of the analysis on the coal blend are given in Table 4. The blend consists of five different seams from a Virginia coal mine. The blend is known as Jewell Smokeless. The structure results of coke piece T are given in Table 5, S in Table 6 and B in Table 7. The summary of the structure results is given in Table 8. The results of the texture analysis are given in Table 9. Table 10 contains the CSR results.

5.1 Analytical test results on coal

Table 4: Results of Jewell Smokeless Coal

<u>Proximate Analysis % (Dry)</u>	
Volatile matter	23.81
Ash	6.38
Fixed carbon	69.81
Sulfur % (dry)	0.84
Calorific value (Btu/lb.dry)	14819
(MJ/kg)	34.47
Chlorine % (dry)	0.09
Free Swelling index	9

<u>Giesler Plasticity</u>		
Max. fluidity, ddpm (dial divisions per minute)		2221
Max fluidity temp	°C	446
Softening temp	°C	407
Re-solidification temp	°C	507
Plastic range	°C	100
<u>Ultimate analysis % (dry)</u>		
Carbon		83.72
Hydrogen		4.64
Nitrogen		1.46
Oxygen		2.96
<u>Ash Composition (% in Ash)</u>		
SiO ₂		51.81
Al ₂ O ₃		27.99
Fe ₂ O ₃		10.99
TiO ₂		1.57
CaO		2.01
MgO		1.03
Na ₂ O		0.54
K ₂ O		1.79
P ₂ O ₅		0.45
SO ₃		1.22
Phosphorus (% in coal)		0.0125
Hardgrove Grindability Index		87
<u>Petrographic analysis</u>		
<u>Mean max reflectance% (rank)</u>		1.32
V-type:	10	3
V-type:	11	10
V-type:	12	25
V-type:	13	40
V-type:	14	19
V-type:	15	3
<u>Standard deviation %</u>		0.1

<u>Maceral composition</u>		
<i>Reactives:-</i>		
Vitrinite	%	67.2
Liptenite	%	2.5
Semifusinite	%	1.9
<i>Total Reactives:</i>	%	71.6
<i>Inerts:</i>		
Semifusinite	%	5.8
Micrinite	%	15
Fusinite	%	3.9
Mineral matter	%	3.7
<i>Total Inerts:</i>	%	28.4
Composition Balance Index		1.67
<u>Ash fusion temp °F (reducing atmosphere):</u>		
Initial deformation		2460
Softening		2520
Hemispherical		2560
Flow		2660

5.2 Results of the structural analysis on coke (automated image analysis)

5.2.1 Coke Piece T.

Table 5: Structural properties of coke sample from the top of coke bed the oven: Coke piece T (x is the value and s the standard deviation).

	Sample	Porosity %		Pore diameter μm		Cell wall thickness μm	
		x	s	x	s	x	s
1	TA1	62.8	8.7	18.2	21.2	5.8	22.2
2	TA2	70.8	5.1	21.4	34.2	8.5	37.2
3	TA3	62.5	15.1	17.9	21.9	6.4	22.1
4	TB1	65.9	17.9	12.5	25.0	6.6	18.5
5	TB2	58.4	16.3	13.6	23.0	7.8	19.8
6	TB3	56.5	16.6	14.6	21.2	7.9	18.7
7	TB4	65.8	9.6	21.1	31.0	6.1	23.3
8	TB5	66.8	8.1	15.8	23.7	5.4	18.9
9	TB2-1	71.1	6.2	15.3	18.4	5.0	20.1
10	TC1	69.2	5.9	18.1	18.7	5.2	18.3
11	TC2	68.1	6.0	18.0	31.2	6.2	19.2
12	TC3	42.8	19.3	21.9	60.6	6.0	20.4
13	TC4	71.4	8.0	26.0	29.9	12.0	47.3
14	TC2-1	48.0	16.8	24.3	39.6	5.7	14.4
15	TC3-4	56.0	14.8	15.2	26.2	6.8	17.9
16	TC2-2	61.2	18.7	13.2	22.0	5.9	19.0
17	TD1	66.3	13.1	15.6	29.8	5.5	24.1
18	TD2	70.7	8.8	26.3	29.7	9.0	32.8
19	TD3	62.0	8.6	27.3	36.5	8.9	36.8
20	TD4	71.7	7.1	27.2	31.9	8.5	34.7
21	TD5	72.9	4.3	21.3	33.1	9.3	47.0
22	TD1-1	65.1	6.0	18.9	28.6	8.2	32.2
23	TD2-1	62.3	8.4	21.3	27.7	6.5	23.6
24	TD3-1	68.2	8.7	18.1	19.0	4.2	21.6

25	TD4-1	70.2	6.2	18.9	21.7	8.2	19.8
26	TE1	70.6	5.6	15.0	18.7	5.2	24.0
27	TE2	62.1	5.2	18.8	21.9	8.8	21.1
28	TE3	71.9	7.0	18.5	25.7	8.9	26.0
29	TE4	47.4	18.6	17.4	38.3	6.2	18.2
30	TE5	70.9	8.1	22.3	30.8	6.0	26.8
31	TE1-1	52.9	10.0	20.1	32.7	5.2	20.3
32	TE3-1	59.7	9.6	18.2	31.2	6.6	18.9
33	TF1	70.8	8.4	18.9	22.3	6.2	21.8
34	TF2	64.8	10.7	15.0	19.5	4.9	16.2
35	TF4	72.6	6.3	16.4	20.7	5.0	19.8
36	TF2-1	74.6	5.7	18.6	21.7	8.6	38.3
37	TF3-1	62.1	11.3	18.7	28.6	6.9	22.3
38	TG1	42.8	17.0	20.5	24.1	6.4	25.0
39	TG2	70.9	7.6	26.6	50.8	7.9	38.7
40	TG3	67.3	8.9	22.8	28.9	8.3	21.0
41	TG4	64.5	8.0	26.0	29.9	12.0	47.3
42	TG5	67.0	7.5	11.5	17.1	5.5	17.2
43	TG1-1	62.1	8.1	19.3	31.2	6.9	32.2
44	TG3-1	67.7	8.0	42.7	54.2	11.4	47.7
45	TG2-2	59.3	8.3	20.2	28.1	8.2	21.4
46	TG3-2	59.7	5.9	18.2	22.6	6.6	17.2
47	TG4-2	62.1	7.6	18.2	27.5	8.7	18.2
48	TH1	67.0	6.6	21.5	26.9	6.9	17.0
49	TH2	59.6	10.6	18.5	33.8	6.0	20.2
50	TH3	73.5	7.4	22.2	29.8	5.6	29.0
51	TH2-1	69.7	7.3	20.3	25.4	6.4	22.4
52	TH3-1	67.3	12.0	27.0	40.6	11.0	45.1
53	TI1	67.3	7.8	28.7	36.2	8.9	31.6
54	TI2	62.8	8.1	27.2	32.2	6.1	32.2
55	TI4	61.2	5.1	21.6	31.2	8.1	22.8
56	TI1-1	55.3	8.6	22.6	32.1	9.0	28.5
57	TI2-1	47.7	17.1	17.1	35.8	6.3	15.1
58	TI3-1	65.7	11.9	27.0	44.5	11.8	47.5
59	TI3-2	67.2	5.9	18.8	21.2	5.2	18.2

60	TI2-3	71.8	7.2	16.0	19.8	5.2	20.0
61	TI1-4	61.2	5.2	16.2	18.1	5.2	26.2
62	TJ1	59.0	12.4	18.7	21.5	9.0	23.9
63	TJ2	66.0	16.0	18.7	32.5	8.7	14.9
64	TJ3	62.2	8.2	18.2	18.2	6.2	21.8
65	TJ4	59.8	11.2	20.1	24.2	5.3	18.8
66	TJ1-1	61.8	8.2	17.2	21.4	5.9	18.2
67	TJ2-1	59.7	13.4	19.6	35.7	6.1	21.8
68	TJ3-1	63.9	12.6	13.4	20.9	6.2	30.2
69	TJ4-1	67.5	9.1	17.4	22.4	4.9	17.5
70	TJ1-2	62.7	8.1	18.2	21.8	5.9	18.3
71	TJ2-2	70.0	5.9	18.0	21.8	6.8	21.1
72	TJ2-3	73.7	6.1	18.1	21.7	6.1	23.8
73	TJK1	74.2	6.7	19.3	24.9	6.9	32.1
74	TJK2	56.2	5.7	18.6	21.3	8.6	23.0
75	TJK3	56.0	5.0	21.5	23.6	9.0	27.6
76	TJK4	63.2	8.1	21.3	32.1	9.0	19.9
77	TK1-1	59.1	6.5	21.1	28.6	9.1	18.5
78	TK2-1	68.1	6.5	18.3	21.5	6.1	23.6
79	TK3-1	71.5	7.2	19.7	24.5	5.9	22.9
80	TK4-1	71.2	6.0	20.9	24.4	7.8	29.5
81	TK5-1	66.8	8.1	22.7	30.5	8.0	20.0
82	TK1-2	65.1	9.7	21.5	29.0	7.7	19.7
83	TK2-2	56.9	10.4	17.9	28.7	5.7	18.2
84	TK2-3	70.4	8.1	17.4	23.4	4.9	18.4
85	TK3-3	68.3	6.5	12.2	15.0	5.5	15.6
86	TL1	61.2	8.3	22.3	31.2	8.2	18.2
87	TL2	71.2	12.3	19.7	30.9	5.9	28.2
88	TL3	67.1	7.6	40.7	31.7	14.1	42.1
89	TL4	67.0	12.5	12.7	21.9	5.4	21.6
90	TL5	59.3	8.1	20.2	28.3	8.2	20.1
91	TL6	66.8	9.8	12.7	21.0	5.7	18.4
92	TL1-1	59.5	13.5	38.7	52.0	13.1	45.5
93	TL3-1	71.5	5.7	10.2	12.5	5.4	18.9
94	TL4-1	57.1	8.9	18.2	27.3	6.1	18.1

95	TL2-3	62.1	5.8	11.2	18.2	6.2	18.2
96	TL2-4	59.1	8.9	17.2	30.3	8.1	18.8
97	TM1	68.3	6.5	12.2	15.0	5.5	15.6
98	TM2	63.2	5.9	18.8	21.3	6.2	17.2
99	TM3	59.1	6.2	14.2	18.2	6.9	21.8
100	TM1-1	61.1	5.9	15.8	18.7	54.9	22.0
101	TM1-2	58.5	8.1	19.8	18.9	6.1	18.3
102	TM2-1	67.1	8.2	18.8	21.1	7.9	29.3
103	TM2-2	63.8	9.1	16.0	22.8	6.0	19.1
104	TN1	46.5	11.3	23.7	40.6	5.9	16.0
105	TN2	57.1	8.3	18.8	28.2	5.1	18.8
106	TN3	47.2	18.9	23.8	9.9	9.2	6.3
107	TN1-1	58.2	9.1	18.2	32.1	6.2	17.0
108	TO1	54.5	16.4	24.0	40.2	7.4	25.7
109	TO2	48.3	11.4	41.9	41.3	9.3	30.7
110	TO3	62.2	8.2	18.7	21.8	5.9	17.9
	Total	6978.2	1018.9	2188.1	3004.4	781.4	2627.5
	Mean	63.4	9.3	19.9	27.3	7.1	23.9

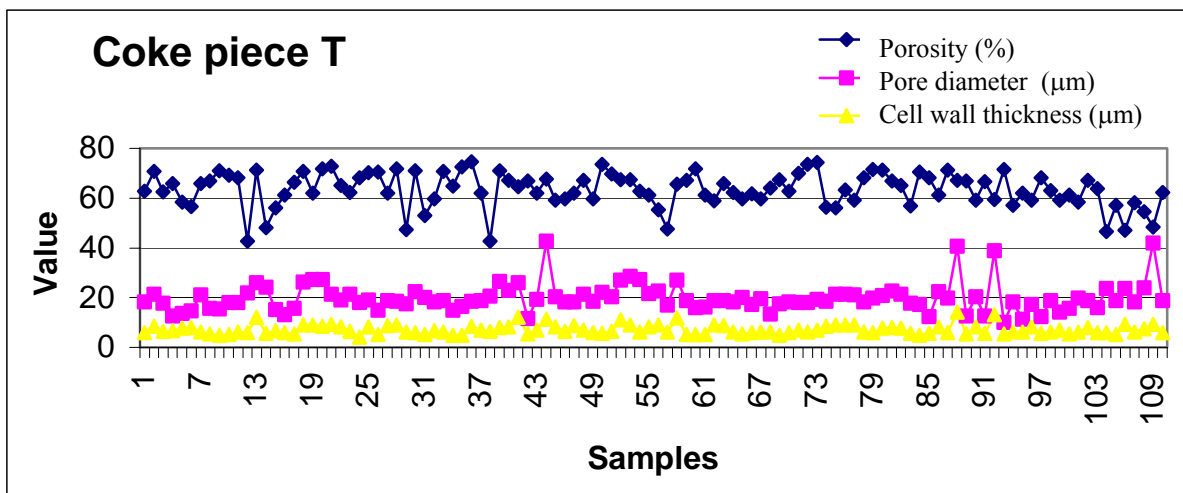
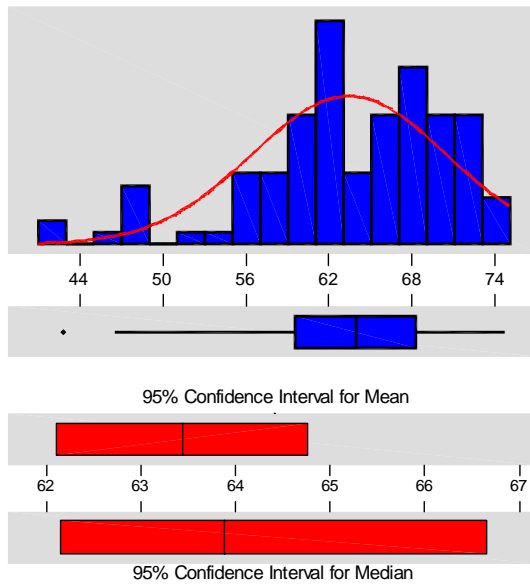


Figure 16: Structural properties of coke piece T.

Descriptive Statistics

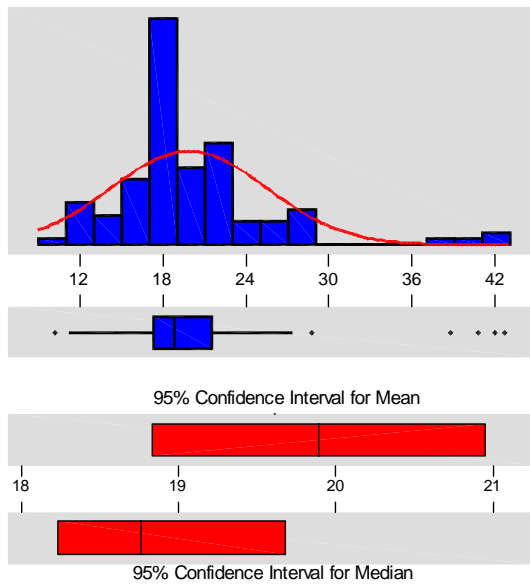


Variable: Porosity

Anderson-Darling Normality Test	
A-Squared:	1.568
P-Value:	0.000
Mean	63.4382
StDev	7.0166
Variance	49.2325
Skewness	-8.6E-01
Kurtosis	0.653627
N	110
Minimum	42.7500
1st Quartile	59.4625
Median	63.8700
3rd Quartile	68.2500
Maximum	74.5600
95% Confidence Interval for Mu	
	62.1122 64.7641
95% Confidence Interval for Sigma	
	6.1960 8.0897
95% Confidence Interval for Median	
	62.1429 66.6456

Figure 17: Descriptive statistics of porosity of coke piece T

Descriptive Statistics

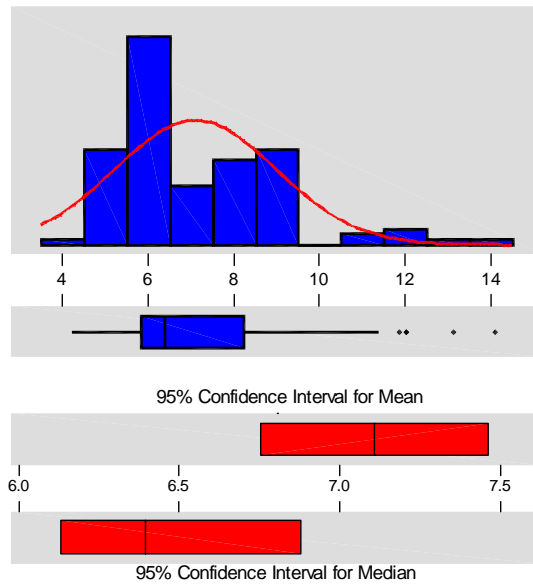


Pore diameter

Anderson-Darling Normality Test	
A-Squared:	4.300
P-Value:	0.000
Mean	19.8919
StDev	5.6198
Variance	31.5821
Skewness	1.87755
Kurtosis	5.55936
N	110
Minimum	10.1600
1st Quartile	17.3150
Median	18.7600
3rd Quartile	21.4500
Maximum	42.6500
95% Confidence Interval for Mu	
	18.8299 20.9539
95% Confidence Interval for Sigma	
	4.9626 6.4793
95% Confidence Interval for Median	
	18.2276 19.6771

Figure 18: Descriptive statistics of pore diameter of coke piece T

Descriptive Statistics



Cell wall thickness

Anderson-Darling Normality Test

A-Squared: 3.833
P-Value: 0.000

Mean: 7.10855
StDev: 1.88556
Variance: 3.55535
Skewness: 1.30785
Kurtosis: 1.87575
N: 110

Minimum: 4.2100
1st Quartile: 5.8400
Median: 6.3900
3rd Quartile: 8.2350
Maximum: 14.0700

95% Confidence Interval for Mu
6.7522 7.4649

95% Confidence Interval for Sigma
1.6650 2.1739

95% Confidence Interval for Median
6.1276 6.8775

Figure 19: Descriptive statistics of the cell wall thickness of coke piece T

5.2.2 Coke Piece S

Table 6: Structural properties of coke sample from the side of the coke bed in the oven:
Coke piece S (x is the value and s the standard deviation).

	Sample	Porosity %		Pore diameter μm		Cell wall thickness μm	
		x	s	x	s	x	s
1	SA1	65.1	8.3	36.4	43.3	13.1	44.5
2	SB1	59.9	13.0	41.0	57.7	11.3	41.5
3	SB1-2	77.6	6.8	12.5	13.8	5.9	25.5
4	SC1	65.9	7.7	36.0	40.4	10.3	38.5
5	SC2	69.2	7.1	14.1	16.8	5.8	17.8
6	SD1	45.3	28.9	35.1	44.9	7.0	27.2
7	SD2	73.1	10.2	6.8	8.8	4.8	18.9
8	SD3	75.0	4.7	10.8	11.9	6.0	20.4
9	SD4	77.7	5.9	8.3	9.0	6.4	22.9
10	SE1	54.5	11.3	40.7	61.1	8.6	31.5
11	SE2	61.2	12.9	32.6	48.9	8.4	35.4
12	SE3	65.8	14.8	23.9	35.6	7.4	28.0
13	SE4	76.7	6.2	25.5	33.2	12.8	55.6
14	SE1-1	71.1	13.0	15.7	27.8	5.6	22.1
15	SE3-1	64.3	12.9	31.6	46.8	9.2	36.6
16	SF1	68.9	9.2	23.7	31.2	6.2	25.3
17	SF2	64.3	15.2	27.9	45.3	7.4	32.1
18	SF3	67.2	10.3	14.9	17.3	6.4	18.3
19	SF4	75.3	6.2	12.7	14.7	6.1	21.8
20	SF3-1	72.4	6.8	12.8	14.7	6.3	19.7
21	SG1	71.1	8.8	19.4	27.2	6.1	28.3
22	SG2	72.5	6.1	16.2	18.8	8.9	28.5
23	SG3	74.7	7.2	17.2	18.5	9.6	32.5
24	SG4	70.5	7.4	27.8	31.6	12.6	40.7
25	SG5	76.7	4.8	10.7	11.9	6.7	23.9
26	SG1-1	75.6	7.7	12.0	18.3	5.7	21.1
27	SG2-1	67.7	13.8	11.2	21.8	5.4	18.5

28	SG3-1	75.1	5.7	13.8	14.6	8.0	25.3
29	SG4-1	81.2	2.5	10.4	10.5	6.6	30.5
30	SG1-2	78.3	5.3	9.1	10.6	5.2	24.1
31	SG2-1	67.7	13.8	11.2	21.8	5.4	18.5
32	SH1	70.6	6.2	22.4	25.3	8.3	27.1
33	SH2	75.7	5.1	12.5	14.0	7.1	24.5
34	SH3	76.2	6.1	19.5	22.4	9.4	35.7
35	SH4	59.0	21.7	20.2	51.9	9.8	33.3
36	SH5	76.0	3.8	10.8	12.0	7.9	26.5
37	SH3-1	75.1	8.1	15.1	12.4	6.9	18.2
38	SH4-1	72.4	8.0	11.1	14.7	5.3	21.5
39	SI1	61.9	8.1	27.5	60.7	15.8	58.5
40	SI2	65.3	9.9	19.0	34.3	10.6	31.2
41	SI3	59.7	11.9	23.2	45.3	10.9	47.9
42	SI4	71.0	8.1	22.1	20.2	10.9	32.2
43	SI5	60.4	13.7	14.7	26.4	7.8	23.0
44	SI6	71.0	12.4	12.6	14.8	6.3	20.0
45	SI3-1	73.0	5.5	11.5	15.2	5.2	18.2
46	SI3-2	72.6	10.9	14.8	25.2	6.5	27.5
47	SI4-1	59.2	12.1	15.0	30.3	5.9	17.9
48	SI4-2	65.9	15.2	13.0	15.3	6.4	21.9
49	SI4-3	67.1	20.7	11.0	17.8	5.4	20.2
50	SI4-4	51.8	12.6	25.0	60.5	7.4	23.6
51	SI5-1	73.1	4.5	13.9	16.4	8.6	26.3
52	SI5-2	78.3	8.0	12.7	18.0	9.3	34.5
53	SI5-3	76.1	5.2	16.3	17.7	9.1	31.6
54	SI5-4	65.4	11.0	9.6	15.8	6.6	20.6
55	SJ1	69.0	11.3	22.8	28.1	8.9	35.3
56	SJ2	58.6	21.8	24.7	43.6	7.3	23.5
57	SJ3	65.9	8.9	19.2	23.4	5.1	18.1
58	SJ4	77.7	3.7	8.9	10.2	6.8	25.7
59	SJ3-1	73.3	4.4	11.0	12.1	5.7	22.1
60	SJ3-2	77.8	3.8	25.2	26.8	12.0	52.8
61	SJ4-1	68.1	9.0	10.2	12.1	5.2	18.7
62	SK1	61.5	10.8	12.7	20.6	6.9	18.7

63	SK2	68.1	9.1	18.0	22.5	7.3	20.9
64	SK3	65.2	11.9	33.2	45.3	10.9	47.9
65	SK4	62.7	8.0	28.2	38.1	7.6	30.2
66	SK5	72.5	6.5	8.4	12.5	4.9	17.2
67	SK6	77.7	11.4	12.1	13.4	5.0	23.9
68	SK5-1	78.8	12.7	10.0	12.4	5.7	23.9
69	SL1	76.4	4.7	19.8	23.7	8.1	36.7
70	SM1	65.1	10.3	18.3	24.8	7.4	27.2
71	SM2	70.6	5.6	13.8	15.5	4.9	18.1
72	SM3	76.6	4.7	19.8	23.7	8.1	36.7
73	SM4	59.7	10.2	16.1	24.8	5.1	17.9
	Total	5063.5	691.5	1328.6	1848.6	555.3	2032.6
	Mean	69.4	9.5	18.2	25.3	7.6	27.8

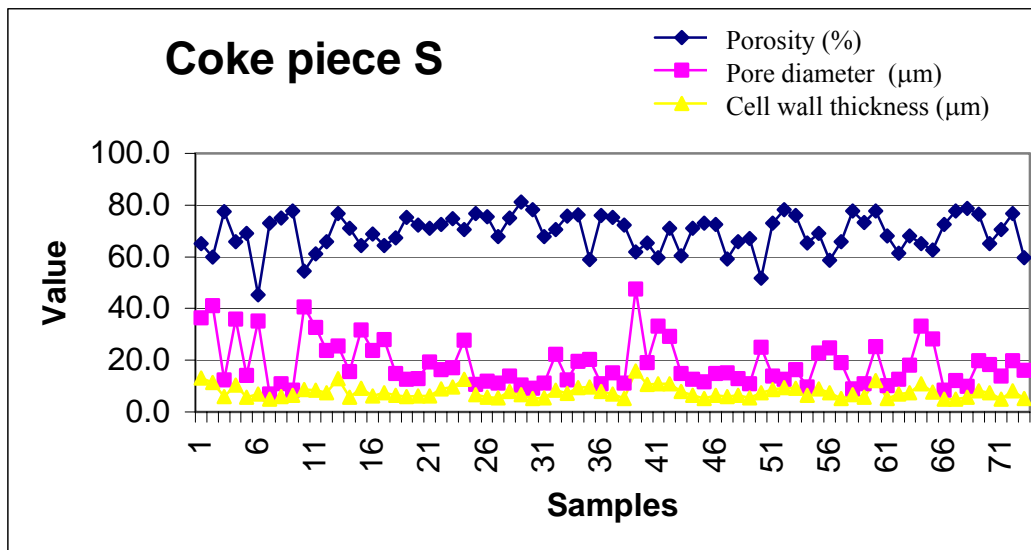
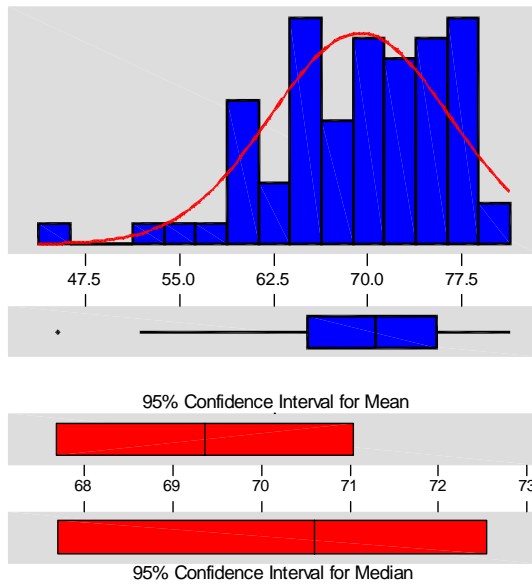


Figure 20: Structural properties of coke piece S.

Descriptive Statistics



Variable: Porosity S

Anderson-Darling Normality Test

A-Squared: 0.980
P-Value: 0.013

Mean 69.3658
StDev 7.1380
Variance 50.9503
Skewness -8.2E-01
Kurtosis 0.680471
N 73

Minimum 45.3000
1st Quartile 65.1500
Median 70.6000
3rd Quartile 75.4500
Maximum 81.2000

95% Confidence Interval for Mu

67.7003 71.0312

95% Confidence Interval for Sigma

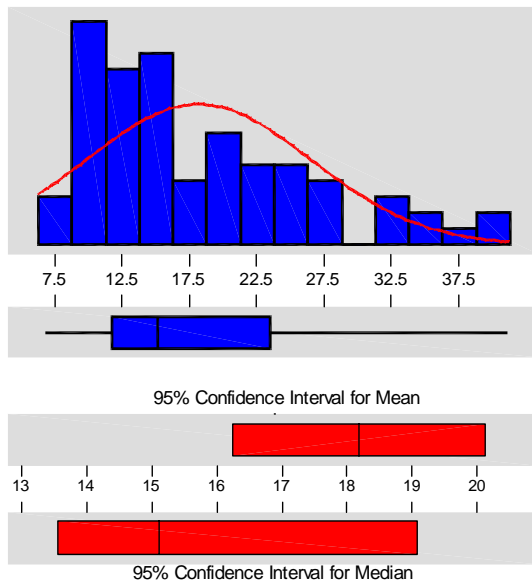
6.1385 8.5291

95% Confidence Interval for Median

67.7000 72.5318

Figure 21: Descriptive Statistics of the Porosity of Coke piece S

Descriptive Statistics



Pore diameter

Anderson-Darling Normality Test

A-Squared: 2.463
P-Value: 0.000

Mean 18.1904
StDev 8.3165
Variance 69.1637
Skewness 1.03037
Kurtosis 0.333863
N 73

Minimum 6.8000
1st Quartile 11.7500
Median 15.1000
3rd Quartile 23.4500
Maximum 41.0000

95% Confidence Interval for Mu

16.2500 20.1308

95% Confidence Interval for Sigma

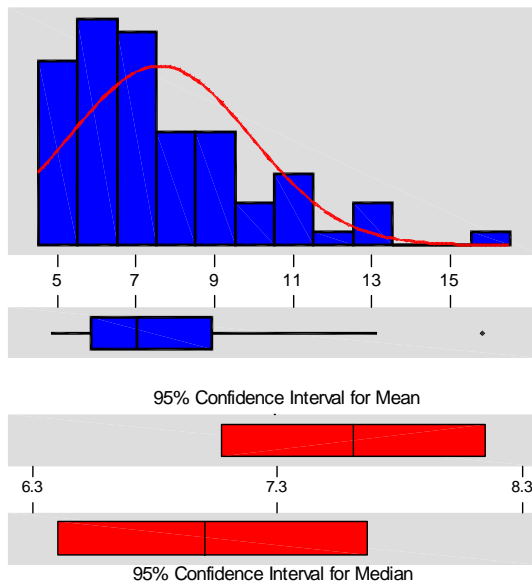
7.1520 9.9373

95% Confidence Interval for Median

13.5459 19.0635

Figure 22: Descriptive statistics of the pore diameter of coke piece S

Descriptive Statistics



Cell wall thickness

Anderson-Darling Normality Test

A-Squared: 2.011
 P-Value: 0.000

Mean 7.60959
 StDev 2.31103
 Variance 5.34088
 Skewness 1.20122
 Kurtosis 1.36517
 N 73

Minimum 4.8000
 1st Quartile 5.8500
 Median 7.0000
 3rd Quartile 8.9000
 Maximum 15.8000

95% Confidence Interval for Mu
 7.0704 8.1488

95% Confidence Interval for Sigma
 1.9875 2.7614

95% Confidence Interval for Median
 6.4000 7.6635

Figure 23: Descriptive statistics of the cell wall thickness of coke piece S

5.2.3 Coke Piece B

Table 7: Structural properties of coke sample from the bottom of the coke bed in the oven: Coke piece B (x is the value and s the standard deviation).

	Sample	Porosity %		Pore diameter μm		Cell wall thickness μm	
		x	s	x	s	x	s
1	BA1	58.9	13.0	21.0	26.4	5.8	17.3
2	BA2	61.5	11.8	18.1	29.3	5.2	18.3
3	BA3	52.4	6.9	20.3	26.6	6.2	28.5
4	BA1-1	54.1	10.2	25.3	44.1	5.3	19.7
5	BA1-2	61.3	14.3	17.0	25.0	6.6	19.5
6	BA1-3	51.3	10.4	38.3	67.0	7.9	29.1
7	BA2-1	59.5	11.1	26.4	33.6	7.9	25.2
8	BA2-2	52.7	13.0	22.9	34.7	9.0	29.9
9	BA2-3	57.6	7.4	15.8	21.2	5.4	19.1
10	BB1	63.9	10.6	28.7	49.3	7.3	31.9
11	BB2	54.1	8.2	42.8	31.8	17.1	25.3
12	BB3	51.8	9.0	37.2	32.8	10.1	21.8
13	BB1-1	50.7	12.7	32.7	53.0	8.5	27.9
14	BB1-2	65.9	9.8	26.7	36.0	7.1	27.4
15	BB1-3	62.5	11.1	27.9	40.5	6.3	26.6
16	BB2-2	57.4	6.4	22.7	30.0	5.5	17.8
17	BC1	57.2	9.1	19.8	27.5	6.0	24.8
18	BC2	63.0	8.5	38.7	54.9	9.0	36.4
19	BC3	57.4	8.4	34.3	48.2	5.7	21.0
20	BC1-1	62.5	9.7	31.1	51.9	8.2	19.0
21	BC1-2	54.9	11.2	31.2	38.2	11.8	18.2
22	BC1-3	63.0	10.7	44.4	54.0	9.7	35.8
23	BC2-2	54.0	7.8	25.5	46.0	5.3	18.4

24	BD1	59.6	10.6	29.9	50.0	6.6	26.5
25	BD2	49.1	14.3	21.2	32.1	9.0	14.3
26	BD3	49.2	7.3	30.2	36.2	8.8	14.2
27	BD1-1	39.0	10.2	39.3	67.9	7.6	29.9
28	BD1-2	53.3	9.3	29.0	50.7	6.0	21.6
29	BD1-3	69.6	7.8	18.2	24.2	6.1	23.9
30	BD2-2	58.4	11.3	26.9	48.2	5.7	22.4
31	BE1	65.5	7.7	30.6	43.6	7.5	31.0
32	BE2	51.6	10.2	45.5	74.5	10.5	37.2
33	BE3	53.5	17.7	19.7	37.4	5.4	17.1
34	BE1-1	58.7	11.2	22.2	41.2	11.2	28.1
35	BE1-2	63.4	10.9	27.2	41.0	7.2	31.0
36	BE1-3	64.4	7.4	23.1	34.3	5.5	21.1
37	BE2-1	49.7	14.2	42.9	70.7	10.1	34.4
38	BE2-2	59.5	7.0	23.2	27.3	6.8	24.9
39	BE2-3	50.1	17.5	42.5	37.2	9.7	34.4
40	BE3-1	57.9	6.9	27.8	7.5	5.4	18.3
41	BE3-2	52.7	12.1	18.2	29.2	8.6	41.5
42	BE3-3	64.3	5.4	27.4	36.6	6.1	25.3
43	BF1	53.0	12.6	28.4	56.2	6.4	23.9
44	BF2	54.2	8.1	23.2	31.8	11.2	14.2
45	BF3	57.2	8.2	26.4	32.8	8.2	18.9
46	BF1-1	45.9	16.7	52.0	85.7	11.0	36.2
47	BF1-2	45.9	12.8	14.2	23.6	5.4	19.3
48	BF1-3	42.9	19.5	32.5	29.6	8.8	18.6
49	BF2-1	64.9	16.4	18.0	42.0	8.4	24.8
50	BF2-3	46.9	10.9	42.0	66.1	9.8	30.3
51	BF3-1	66.1	9.5	42.1	46.3	12.2	42.7
52	BF3-3	58.5	11.6	34.8	63.4	6.4	27.8
53	BG1	56.7	8.5	23.7	37.8	5.8	21.0
54	BG2	52.3	9.5	31.2	54.6	7.0	24.6
55	BG3	67.4	10.3	28.0	43.0	5.5	17.1
56	BG4	63.8	10.4	28.3	37.0	6.1	23.0
57	BG1-1	54.3	12.8	28.4	54.6	6.4	24.1
58	BG1-2	50.6	7.1	37.2	40.4	5.7	48.3

59	BG1-3	47.5	11.4	32.0	57.6	5.5	18.6
60	BG2-1	49.4	14.0	28.8	50.7	5.3	17.6
61	BG2-2	50.9	8.0	34.4	47.2	8.3	22.0
62	BG2-3	41.8	15.8	37.6	68.9	6.5	20.2
63	BG3-1	46.9	14.4	31.1	52.5	5.5	17.6
64	BH1	61.8	5.5	29.5	38.8	6.6	24.5
65	BH2	53.2	6.9	29.0	30.3	12.2	49.1
66	BH3	55.0	8.0	37.7	50.9	10.5	53.8
67	BH4	39.5	17.2	37.5	71.9	6.6	22.1
68	BH1-1	47.2	11.7	26.1	48.3	8.1	21.8
69	BH1-2	43.9	10.4	28.0	55.6	5.2	15.4
70	BH1-3	64.8	8.3	28.1	42.4	13.1	49.8
71	BH2-1	47.6	8.3	30.0	24.9	6.2	26.5
72	BH2-2	49.6	13.4	18.0	57.9	5.7	20.8
73	BH2-3	58.6	10.2	26.8	44.7	7.0	21.3
74	BI1	60.0	7.0	25.0	28.0	6.6	20.7
75	BI2	47.2	13.5	22.0	52.8	9.8	27.8
76	BI3	59.7	10.2	40.1	35.0	8.0	27.5
77	BI1-1	54.0	9.2	24.8	32.9	5.8	18.7
78	BI1-2	51.1	8.1	23.8	40.9	6.1	18.9
79	BI1-3	45.7	10.6	26.3	37.7	13.7	50.9
	Total	4352.9	837.1	2300.5	3406.0	608.8	2036.4
	Mean	55.1	10.6	29.1	43.1	7.7	25.8

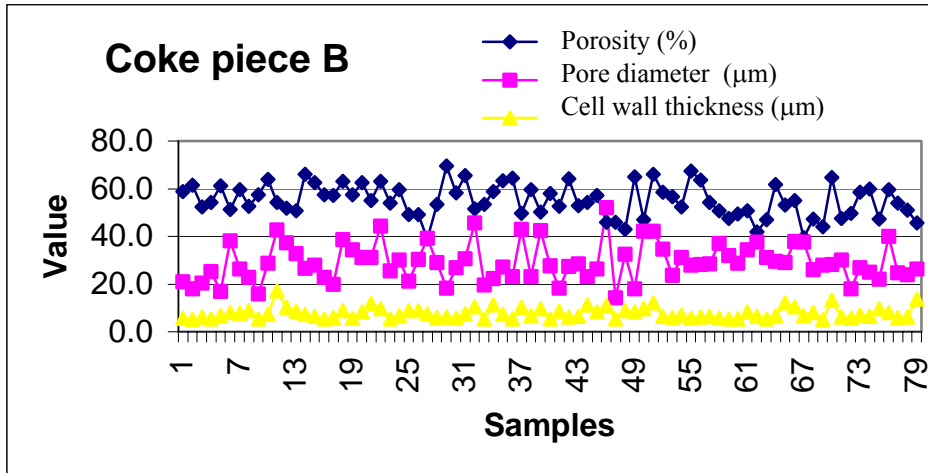


Figure 24: Structural properties of coke piece B.

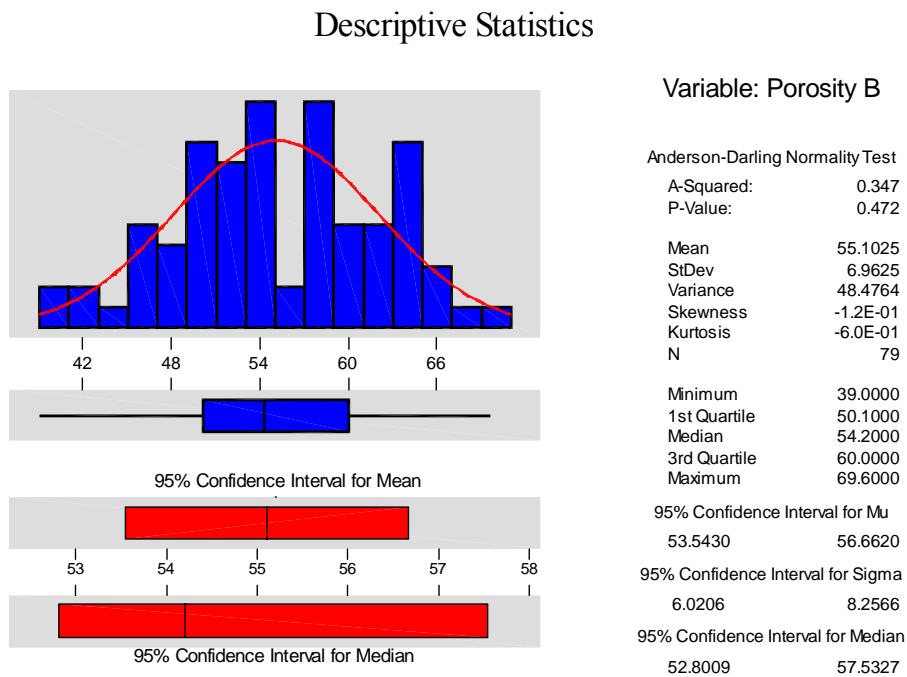
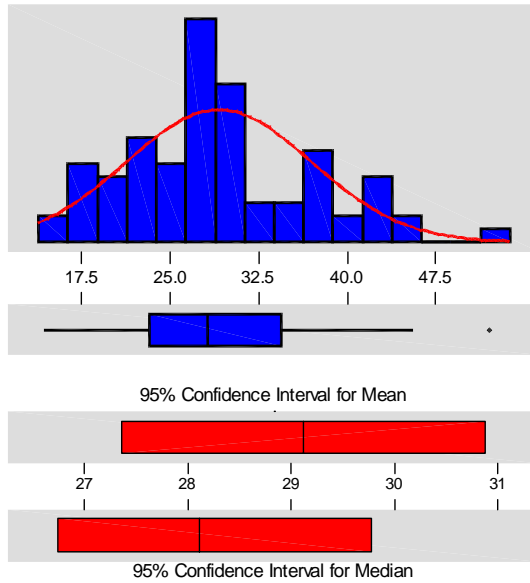


Figure 25: Descriptive statistics of porosity of coke piece B

Descriptive Statistics



Pore diameter

Anderson-Darling Normality Test

A-Squared: 0.791
P-Value: 0.039

Mean 29.1241
StDev 7.8517
Variance 61.6498
Skewness 0.522975
Kurtosis -2.9E-02
N 79

Minimum 14.2000
1st Quartile 23.2000
Median 28.1000
3rd Quartile 34.3000
Maximum 52.0000

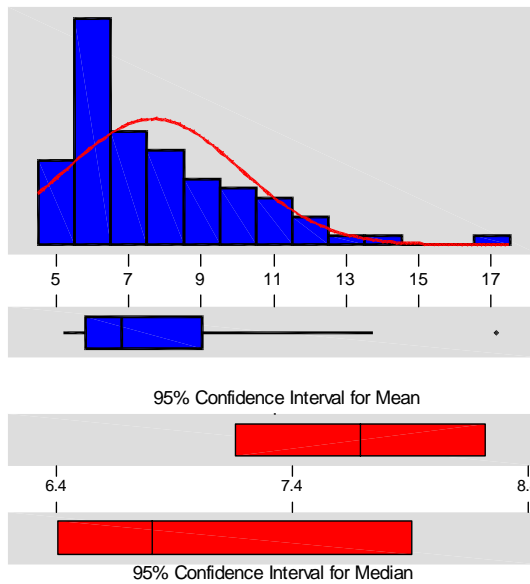
95% Confidence Interval for Mu
27.3654 30.8827

95% Confidence Interval for Sigma
6.7895 9.3111

95% Confidence Interval for Median
26.7336 29.7655

Figure 26: Descriptive statistics of the pore diameter of coke piece B

Descriptive Statistics



Cell wall thickness

Anderson-Darling Normality Test

A-Squared: 3.017
P-Value: 0.000

Mean 7.68734
StDev 2.37635
Variance 5.64702
Skewness 1.40306
Kurtosis 2.26787
N 79

Minimum 5.2000
1st Quartile 5.8000
Median 6.8000
3rd Quartile 9.0000
Maximum 17.1000

95% Confidence Interval for Mu
7.1551 8.2196

95% Confidence Interval for Sigma
2.0549 2.8180

95% Confidence Interval for Median
6.4000 7.9000

Figure 27: Descriptive statistics of the cell wall thickness of coke piece B

Table 8: Summary of structure results

Coke Piece	Porosity		Pore diameter		Cell wall thickness	
	%		µm		µm	
	Mean	StDev	Mean	StDev	Mean	StDev
T	63.4	9.3	19.9	27.3	7.1	23.9
S	69.4	9.5	18.2	25.3	7.6	27.8
B	55.1	10.6	29.1	43.1	7.7	25.8

StDev – Standard deviation

5.3 Results of the texture analysis on coke (point counting)

The texture analysis is based on the point counting of individual carbon phases. Two pellets of each sample were point counted. The results are given in Table 9:

Table 9: Texture results of coke pieces T, S and B.

	Sample T		Sample S		Sample B	
	Cauliflower	Tar	Cauliflower	Tar	Cauliflower	Tar
Isotropic vitrinoke	0	0.1	0	0	0	0
Anisotropic						
Fine Mosaic	0	0	0	0	0	0
Medium Mosaic	1.6	0	4	2.2	0	0
Coarse Mosaic	8.7	8	7.7	9.8	13.4	12.7
Lenticular	56.2	56.1	52	52	47.8	52.2
Ribbon	15.6	14.2	13.6	12.8	11.9	13.2
Isotropic Inertinoke	3.2	0.4	2.2	1.5	4	3.5
Anisotropic Inertinoke	11.5	16.2	13.7	14.7	18	14.3
Pyrolytic Carbon	1.2	1.8	3.6	3.4	0.2	0.2
Mineral matter	2	3.2	3.2	3.6	4.7	3.9

5.4 Results of the CSR tests on coke

Table 10: CSR results

Sample	CSR value
Sample T: Cauliflower zone	60.5
Middle zone	60.4
Sample B: Middle zone	63.7
End zone	64.7
Sample S: Middle zone	65

6. DISCUSSION

6.1 Results of the structural analysis

The standard deviation of the individual values is very large, sometimes as much as twice or nearly three times the actual value. However, this is a characteristic of coke as the pores are normally very irregularly shaped.

Since the texture analysis and the CSR results apply to the cauliflower and tar ends of a specific coke piece, the structural results were also divided into these two zones. Due to the sample labeling system used, the first samples were closest to the cauliflower end. The layers were all about the same size, so that the last samples in the tables represented the coke closest to the tar end. By dividing the list of samples in half, it would represent the cauliflower half and the tar half of the coke piece. Therefore, the mean values for the cauliflower, and tar zones could be calculated. The porosity of the cauliflower and tar zones of each of the 3 coke pieces is graphically displayed in Figure 28.

According to Table 8, the highest porosity values are found in S, the coke from the side of the coke bed. The lowest porosity results are found in B, the coke from the bottom of the coke bed. This is probably due to the weight of the burden that would inhibit swelling.

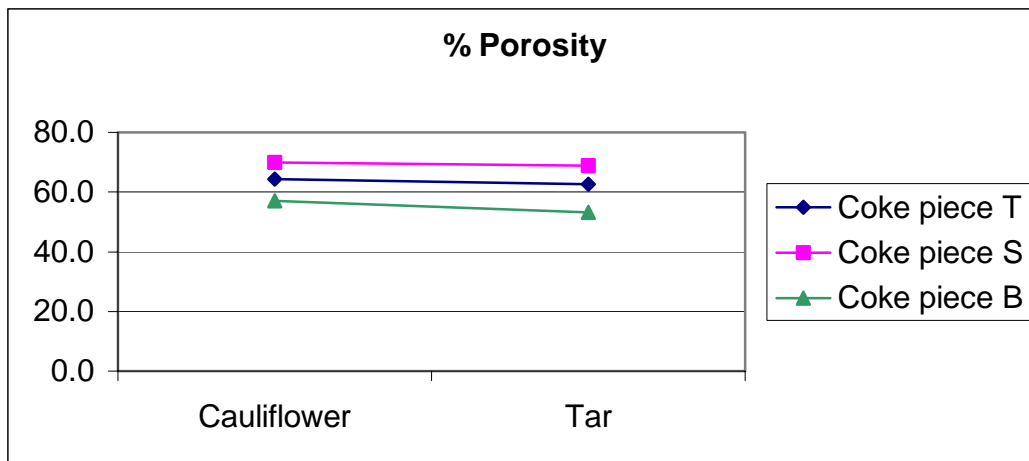


Figure 28: Mean porosity for the cauliflower and tar zones in each coke piece.

The porosity of the cauliflower and tar ends of each coke piece is shown in a box plot in Figure 29. Each population of data is displayed by an outer, rectangular box, and two vertical “whiskers” connected to the box. The bottom whisker represents the first quartile of the data. The box represents the second and third quartiles of the data (50% of the total distribution) and the top whisker represent the fourth quartile of the data. Any outliers would be identified with a *, but there were no outliers identified in these data populations. The horizontal line in the middle of the box represent the median value. The taller the box and whiskers, the more variation exists in the data group. Since all the boxes are fairly equal in size, the distribution of the data were the same for all three the coke pieces. The smaller box within each of the boxes, indicate the 95% confidence interval for each data population.

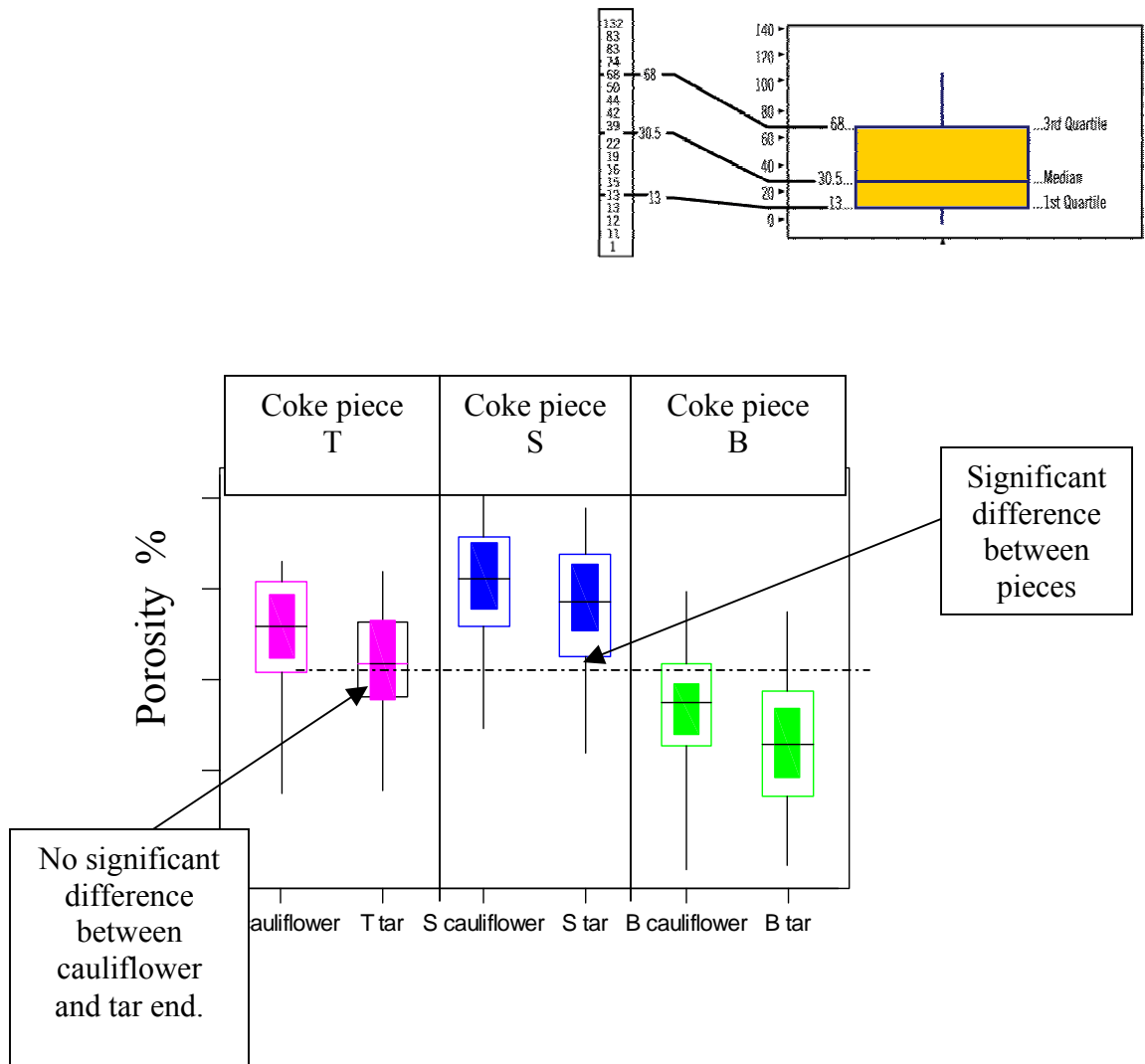


Figure 29: Box plots of porosity of the 3 coke pieces.

If a horizontal line can be drawn from the bottom of one box to the top of the next box, it shows a statistically significant difference between the data populations. According to the box plot in Figure 29, there are significant differences between coke pieces S, T and B. "Statistically significant difference" means that the difference between two groups is a real difference and not likely to be due to sampling error. Therefore if another sample is taken from the same area in the oven, it would likely have similar results.

Sample B contains the thickest cell walls (Figure 32 and 33). The thick cell walls result in a strong framework that would not crack or break easily. It would also be able to withstand the weight of the iron ore in the blast furnace.

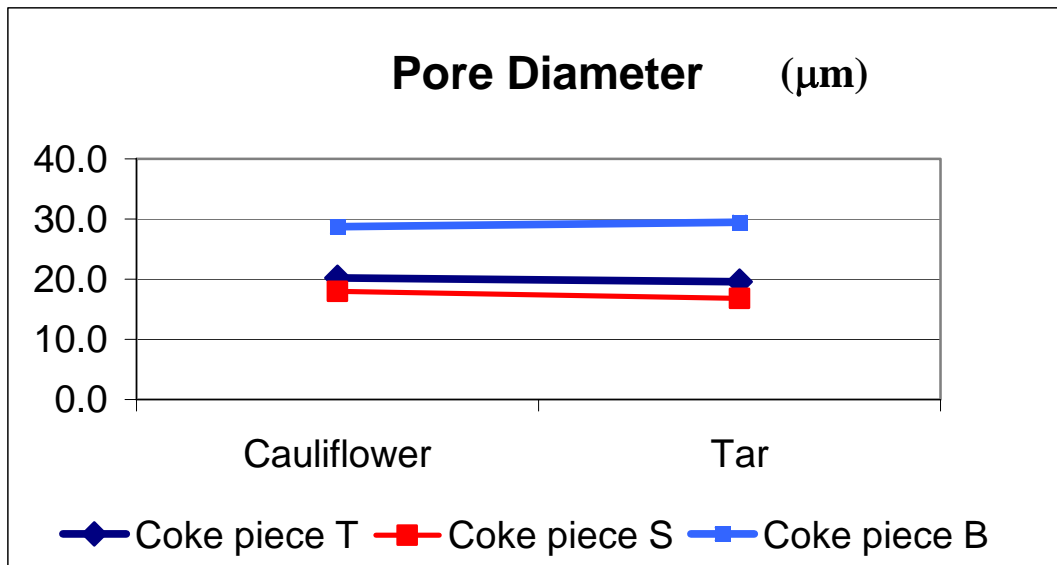


Figure 30: Pore results of the 3 coke pieces.

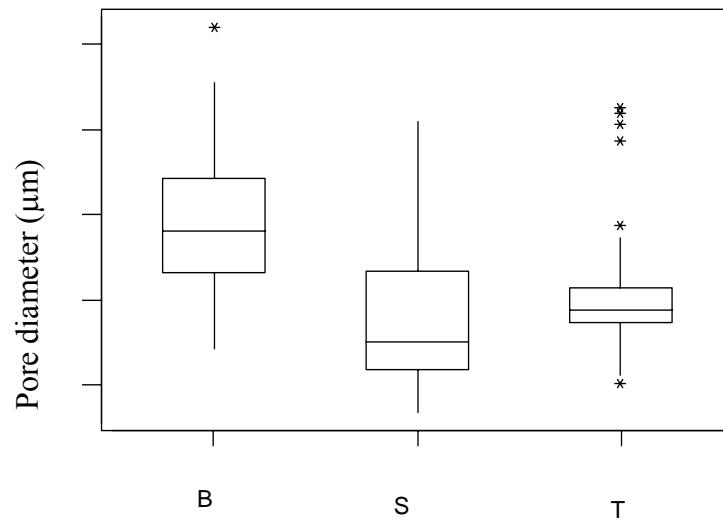


Figure 31: Box plot of the pore diameter of each coke piece investigated.

The * indicates statistical outliers.

According to the box plot, the pore diameter of coke piece B is significantly different from the remaining two coke pieces. It is interesting that the statistical program used to create these boxes plots, recognizes only a narrow distribution of data in the cell wall thickness of coke piece T and identifies the rest of the data as outliers outside the normal distribution pattern.

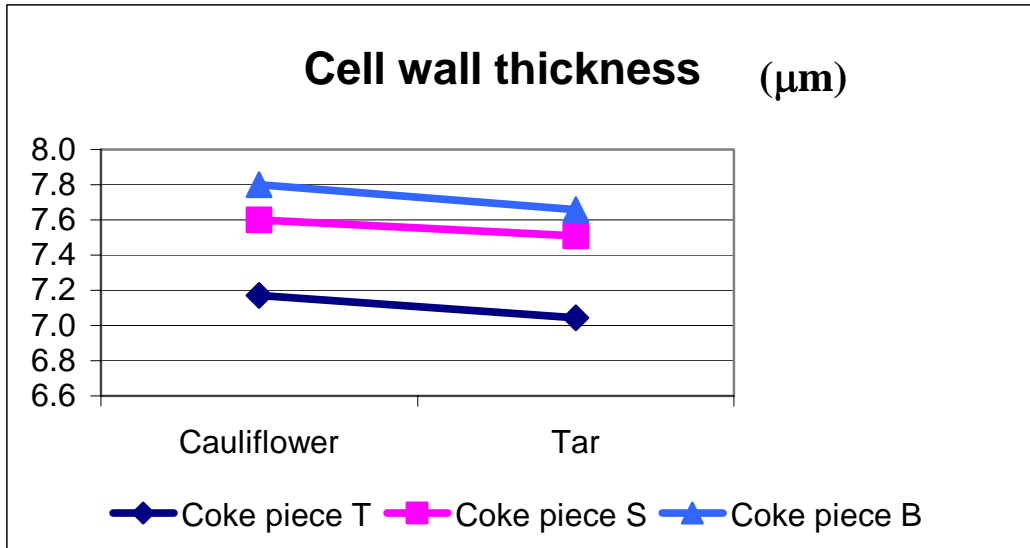


Figure 32 Cell wall thickness as represented by the mean value of each zone of each coke piece investigated.

The largest pore diameter is found in coke piece B from the bottom of the coke oven. The larger pore diameter would allow gas to travel through the coke in the coke oven and also when it is used in the blast furnace. The Porosity is calculated from the pore diameter and cell wall thickness. Although coke piece B contains the largest pore diameter, it also contains the thickest cell walls and the lowest porosity of the 3 pieces that was investigated.

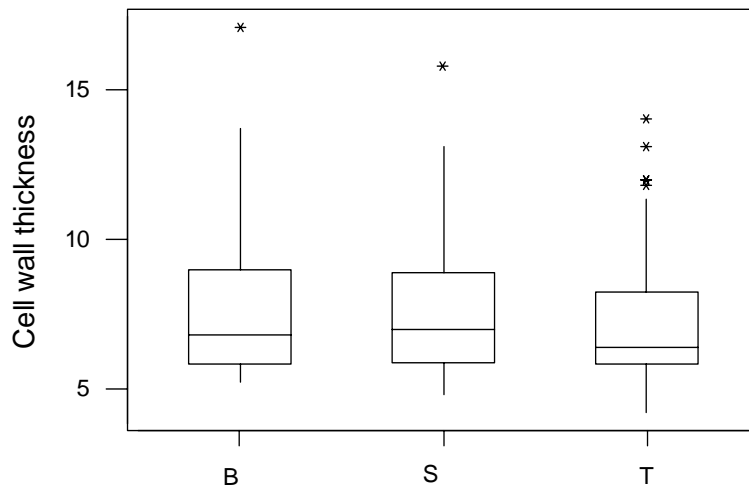


Figure 33: Box plot of the cell wall thickness (μm) of each coke piece investigated.

6.2 Results of the texture analysis

The texture of the coke is a result of the type and rank of coal used to make the coke. Since the oven charge was a homogeneous coal blend, the position of the sample in the oven does not make a big difference in the texture. All the samples therefore show similar results. The only notable difference is in the amount of pyrolytic carbon. Sample S shows the highest amount of pyrolytic carbon. This is an indication of more gas flowing through the side of the coke bed, since the pyrolytic carbon is deposited from volatiles liberated during carbonization.

6.3 CSR Results

As indicated in Table 10, the highest CSR values are found in piece S, which is from the side of the oven. The comparison between the CSR, porosity and percentage pyrolitic carbon is given in Figure 34. Sample S seem to have the highest value for the CSR, the porosity and the pyrolitic carbon.

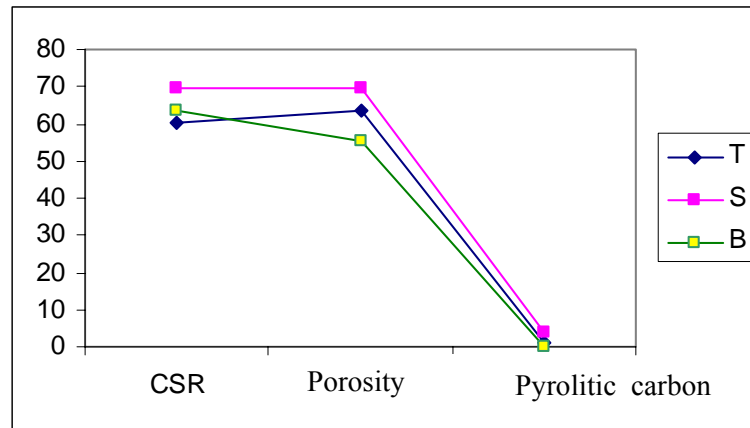


Figure 34: CSR, porosity and pyrolitic carbon results.

A direct correlation was found between the pyrolitic carbon content and the CSR in a study of the cracking reactions in a pilot scale coke oven (Arendt et al 1999). The present study, on coke from a full-scale bee-hive oven, shows that the highest pyrolitic carbon and the highest CSR are found in the coke piece S from the side of the oven, but the lowest pyrolitic carbon value (coke piece T) is not associated with the lowest CSR value (coke piece B) as would have been expected. Instead, the lowest pyrolitic carbon is found in the bottom layer, (coke piece B) but the lowest CSR is found in the top layer. Perhaps these results can be explained by the influence of the structure of the coke. The “bottom coke” has the lowest porosity but the biggest pore diameter and the thickest cell walls. The thick cell wall would be due to the load of coal and the big pore diameter would be a result of the gas passing through the bottom layer. This structure would enhance the CSR so that the CSR value for the bottom coke is higher than would have been expected if only the pyrolitic carbon had been responsible.

The present results indicate that the best quality coke is found on the sides of the oven. While more data will be required to statistically confirm these tentative conclusions, it would seem as if the gas is enhancing the coke quality along the sidewalls. This suggests that the coke from the sides of the ovens can be mechanically separated after the coking cycle by inserting a separating blade when the coke is pushed from the oven. Then the coke could be marked as two distinct grades suggesting an ultra-high quality grade with higher CSR for use in the larger blast furnaces and a high-grade coke for use in the smaller blast furnaces.

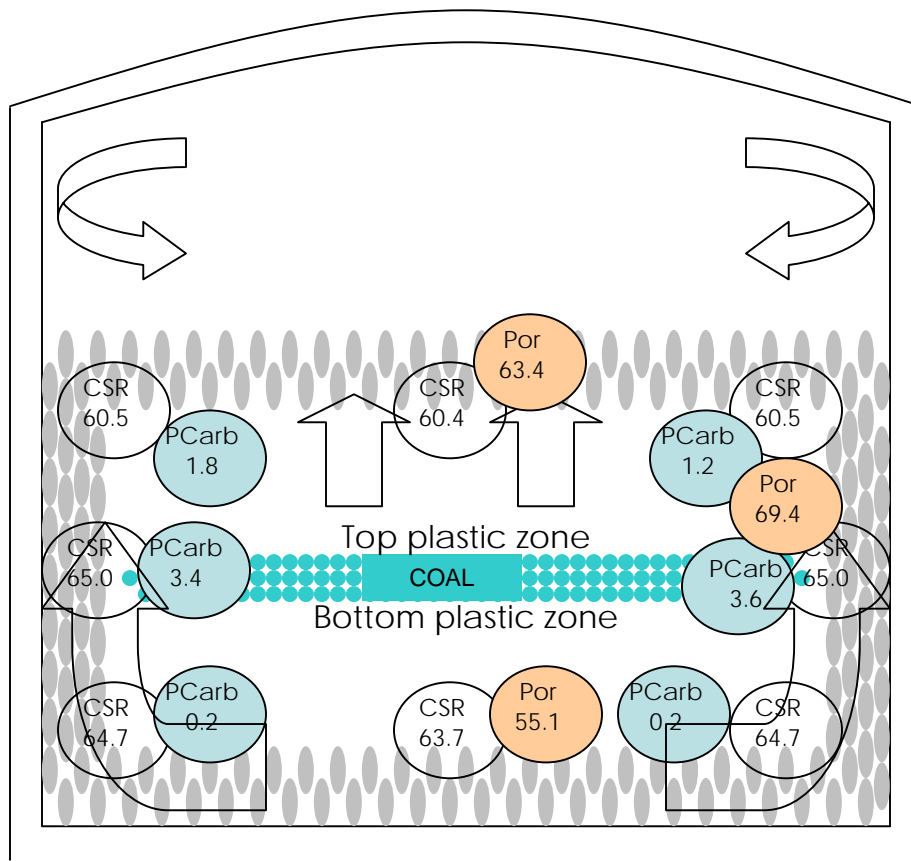
6.4 Coke oven model

As the coal is transformed into coke, the coal at the top and the bottom of the coal bed is closest to the heating zones and first undergo carbonization. Two plastic zones start, one at the top and one at the floor layer of the coal bed and migrate downward from the top, and upward from the bottom. As the plastic zones migrate through the coal, the semi-coke that forms shrinks, fissures are formed, and the semi-coke is transformed into coke. The two plastic zones would finally meet in the middle and all the coal would be transformed into coke after 48 hours.

Based on the experimental data, it has been considered that gas builds up in the plastic zone and flows through fissures in the semi-coke mass. The gas cannot move through the plastic zone (Rhode, W. 1999). With these data in mind, a model of the carbonization process and gas flow in the heat recovery ovens is proposed in an attempt to explain the differences in the coke quality (Figure 35).

For the bottom half of the oven, the gas is forced to move along the floor and up the sides of the oven wall, since the gas would not be able to move through the half molten coke/coal in the plastic zone. The coke on the top of the bed and along the walls of the oven would be exposed to considerably more raw gas than the coke on the floor. The coke on the side

of the oven would be receiving the most exposure to the raw gas since all the raw gas from the floor would move through this part of the oven. The results are that the “side wall” coke and the “top” coke receive heightened exposure to pyrolitic carbon deposition. The data shown in Table 6 confirms that the amount of pyrolitic carbon is higher in the samples from the side and top of the bed than in samples from the bottom.



CSR - CSR Por - Porosity (%) PCarb - Pyrolitic carbon (%)

Arrows show the flow of the raw gas.

Figure 35: Suggested coke oven model with the flow of gas. Gas cannot flow through the plastic zone and is forced from the bottom of the oven up along the sides of the oven.

7. CONCLUSIONS

The study has shown that there are definite spatial variations in coke quality in the beehive coke oven. The flow of raw gas enhances the quality of the coke of the sides along the oven.

The following observations are of relevance:

- Porosity variation: The porosity is significantly higher along the sides of the oven.
- Cell wall thickness: Perhaps due to the weight of the charge in the oven, the cell wall thickness is the highest in the coke that formed on the bottom of the oven.
- Pore diameter: No significant difference exists in pore diameter of coke formed at different parts in the oven.
- Pyrolytic carbon is highest in the coke formed along the side of the oven.
- Highest CSR values are also found in the coke formed along the side of the oven.
- The texture does not vary in different locations in the oven as the oven charge is a homogeneous blend of coal.

It is recommended that:

1. Continued testing is done to statistically confirm the present results.
2. The means to mechanically separate the coke during pushing from the oven is investigated, so that a high and an ultra-high coke quality product can be separated.
3. The quality requirements of the customers are investigated so that the ultra-high quality coke can be used in the bigger blast furnaces and the good quality coke in the smaller furnaces.

ACKNOWLEDGMENTS

I would like to thank both my professors, Prof Johan de Villiers and Prof CP Snyman from the University of Pretoria, South Africa, for their guidance.

I also would like to give special thank you to David Pearson of Pearson Coal Petrography for the use of the facilities.

Marge and Allen Ellis for their technical assistance and support.

Finally I would like to thank my family for their love and support.

8. REFERENCE:

- Ailor, D.C., (1997). Principal environmental issues facing the U.S. coke industry into the 21st century. 1st McMaster's Cokemaking course. McMaster's University, Hamilton, Ontario, Canada. 6.1-6.58.
- American Society for Testing and Materials (ASTM), (1996). Annual book of ASTM Standards.
- Arendt, P, Kuhl H, Huhn F. (1999). Cracking reactions in coke ovens and their importance for coke quality. Training manual, Sun Coke Company Steel course on petrography 2000. pp 22-47.
- Buss W.E., Merhof M.A., Piduch H.G, Schumacher R, Kochanski U. (1999). The Thyssen Still Otto/PACTI non-recovery cokemaking System. 58th Ironmaking Conference, Chicago IL. pp 201-211.
- Ellis, A.R, Schuett, K.J, Thorley, T. and Valia, H.S. (1999). Heat recovery cokemaking at Indiana Harbor Coke Company – An historic event for the steel industry. 58th Ironmaking Conference, Chicago IL. pp 173-186.
- Ellis, C.E and Pruitt, W., (1999). Ten years of maintenance and operation of Jewell Non-recovery ovens. 58th Iron making Conference.
- Ellis and Pruitt (1999)
- Falcon, R.M.S and Snyman C.P., (1986). An Introduction to coal petrography: Atlas of petrographic constituents in the bituminous coals of Southern Africa. Geological Society of South Africa., Review paper No.2.
- Gray, R.J., (1997). Yesterday and tomorrow in coke making. 1st McMaster's Cokemaking course. McMaster's University, Hamilton, Ontario, Canada. 1.1-1.26.
- Gray, R.J., (1985). Coke Carbon Forms: Microscopic Classification and industrial applications. United States Steel Corporation Research. UEC Coal Petrography Short Course, Pennsylvania 1999.

- Greeff, S.C., (1988). 'n Petrografiese ondersoek van kooks berei uit steenkoolmengsels veral met verwysing na Soutpansberg mengsel. * Universiteit van Pretoria
- Keagi, D.D. (1981). Predicting coke stability from coal petrographic analysis. Proc. AIME Ironmaking Conf., 40. 381-392.
- Kolijin, C. (1997). International Coke making issues. 1st McMaster's Coke making course. McMaster's University, Hamilton, Ontario, Canada. 4.1-4.16.
- Leeder W.R., Ryan B.D., Price J.T., and Granden J., (1999). The effect of coal preparation on coke quality. 58th Ironmaking Conference, Chicago IL. pp 215-226.
- Poveromo, J.J., (1997). Coke in the blast furnace. 1st McMaster's Cokemaking course. McMaster's University, Hamilton, Ontario, Canada. 2.1-2.56.
- Price, J., Granden, J., and Hampel, K., (1997). Microscopy, chemistry and rheology tools to determine coal and coke characteristics. 1st McMaster's Cokemaking course. McMaster's University, Hamilton, Ontario, Canada. 4.1-4.74.
- Rhode, W., (1997). Theory of carbonization. 1st McMaster's Cokemaking course. McMaster's University, Hamilton, Ontario, Canada. 7.1-6.18.
- Rhode, W., (1999). Theory of carbonization. 2nd McMaster_Cokemaking course, McMaster's University, Hamilton, Ontario, Canada. Vol. 1, 1999, lecture # 8.
- Shaw I.A.C., (1999). Environmental issues facing the coke making industry into the 21st century. McMaster's University, Hamilton, Ontario, Canada. Vol. 1, 1999, lecture # 8.
- Stach, E., Mackowsky, M.-Th., Teichmuller, M., Taylor, G.H., Chandra, D. and Teihmuller, R. (1982) Stach's textbook of coal petrology. Borntraeger, Berlin.
- Valia, H.S., (1992). Coal and Petroleum Coke Interactions During Carbonization. ISS-AIME Proc., Vol. 51, 1992, pp. 435-447.

- Van Krevelen, D.W., (1961). Coal Typology-Chemistry-Physics-Constitution. Elsevier, Amsterdam.
- Walker, D.N., (1996) High CSR Coke from Non-Recovery Coke making process. 3rd International Coke making congress in Ghent, Belgium, pp 1-5.
- Walters E. B., (1999) The Thyssen Still Otto/PACTI Non-Recovery Coke making system. Iron making Conference Proceedings 1999.p 201 – 214.